INCORPORATION OF SUSTAINABILITY AND ECONOMIC CONSIDERATIONS IN PROCESS CONTROL OF HYDRAULIC FRACTURING IN UNCONVENTIONAL RESERVOIRS

A Thesis

by

PRISCILLE IRENE FLAVIENNE ETOUGHE

Submitted to the Office of Graduate and Professional Studies of
Texas A&M University
in partial fulfillment of the requirements for the degree of

MASTER OF SCIENCE

Chair of Committee,	Joseph Sang-II Kwon
Committee Members,	Mahmoud M. El-Halwagi
	Peter P. Valko
Head of Department,	Efstratios N. Pistikopoulos

August 2018

Major Subject: Energy

ABSTRACT

Typically, the term shale oil refers to natural oil trapped in rock of low porosity and ultra-low permeability. What has made the recovery of shale oil and gas economically viable is the extensive use of hydraulic fracturing. Research on the relationship between the distribution of propping agent, called proppant, and well performance indicates that uniformity of proppant bank height and suspended proppant concentration across the fracture at the end of pumping determines the productivity of produced wells. However, it is important to note that traditional pumping schedules have not considered the environmental and economic impacts of the post-fracturing process such as treatment and reuse of flowback water from fractured wells.

Motivated by this consideration, a control framework is proposed to integrate sustainability considerations of the post-fracturing process into the hydraulic fracturing process. In this regard, a dynamic model is developed to describe the flow rate and the concentration of total dissolved solids (TDS) in flowback water from fractured wells. Then, a thermal membrane distillation (TMD) system is considered for the removal of TDS. A multi-objective problem is formulated to optimize the entire superstructure that consists of hydraulic fracturing, storage, transportation, and water treatment, minimizing annualized cost from recovered water per period and the water footprint of the process. The capabilities of the proposed approach are illustrated through the simulation of different scenarios that are performed to examine the effects of water availability on the productivity of stimulated wells. Finally, the impact of flowback water generation is evaluated using TRACI, a tool for the reduction and assessment of chemical and other environmental impacts.

ACKNOWLEDGEMENTS

First, I would like to thank my advisor Professor Joseph Kwon for his continuous support, patience, and motivation. His guidance and endless contribution helped me through the research and writing of this thesis. At times when I doubted myself, he reinforced in me that when there is a will, the sky is not the limit but the starting point. I wish to thank the members of my dissertation committee: Professor Mahmoud El-Halwagi and Professor Peter Valko for generously offering their time, guidance, and immense knowledge throughout the review of this thesis research. I am profoundly grateful to my research group: Prashanth Siddhamshetty, Rajib Mukherjee, and Kaiyu Cao for their invaluable help and endless support.

I would also like to thank the faculty and staff of the Texas A&M Energy Institute for providing me with excellent educational tools through the course of my Master's program and for the acquired knowledge that will help me make a difference in a world where energy is rapidly transforming. Heartfelt gratitude to my fellow Aggies: Trisha Garcia, Caitlin Carter, Mary Cordes, Kishan Panduranga, Sajjad Haider, Geovani Susanto, Ryan Hallowell, and Sunday Kumuyi. Thank you for the endless laughs, support, and for making the past 10 months a memorable and meaningful experience.

Finally, I must express my profound gratitude to my family. To my parents Pierre and Juliette Etoughe: you have taught me the importance of hard work, perseverance, and determination. Thank you for all of the sacrifices you have made and continue to make for me to fulfill my dreams. Your unconditional love, unflinching support, and words of wisdom have shaped me into the woman I am today.

To my siblings Pascale, Pierrick, Patrick, Philippe, Pierrelyne, and Prunella: thank you for the continuous encouragement and for always making me laugh through the hard and stressful times. To my boyfriend, Roger, thank you for your love and unfailing support throughout the years, and especially through the research and writing process of my thesis. To my son Mason: you are my strength and source of motivation. Thank you for your unconditional love and for inspiring me to become the extraordinary woman I have dreamt of one day becoming.

CONTRIBUTORS AND FUNDING SOURCES

Contributors

This work was supervised by a thesis committee consisting of Professor Joseph Kwon and Mahmoud El-Halwagi of the Artie McFerrin Department of Chemical Engineering and Professor Peter Valko of the Harold Vance Department of Petroleum Engineering.

All work for the thesis was completed by the student.

Funding Sources

Graduate study was financially supported by the student's parents.

NOMENCLATURE

Abbreviations

TDS	Total dissolved solids
TMD	Thermal membrane distillation
TRACI	Tool for reduction and assessment of chemical and environmental impacts
TSS	Total suspended solids
NORM	Naturally occurring radioactive materials
MILP	Mixed-integer linear programing
MPC	Model predictive control
MINLP	Mixed-integer non-linear programing
GAMS	General algebraic modeling system
TAC	Total annual cost
TOC	Total operating cost
TCC	Total capital cost
PI	Productivity Index
EPA	Environmental Protection Agency
CAS	Chemical Abstract Service
COD	Chemical Oxygen Demand
BOD	Biological Oxygen Demand

Parameters

$F_t^{well\_out}$	Flowrate leaving the fracturing well at time period *t*
$C_t^{well\_out}$	TDS concentration leaving the fracturing at time period *t*
H^{time}	Time conversion unit
K	Factor used to annualize the inversion
$V_t^{storage\_initial}$	Initial volume in storage unit at time period *t*
$C_t^{capacity\_disposal}$	Maximum TDS weight fraction in TMD system at time period *t*
$VC_t^{storage}$	Variable cost of interim storage unit at time period *t*
$VC_t^{disposal}$	Variable cost of disposal unit at time period *t*

VC_t^{reuse}	Variable cost of reuse unit at time period *t*
$FC_t^{storage}$	Fixed cost of interim storage unit at time period *t*
$FC_t^{disposal}$	Fixed cost of disposal unit at time period *t*
FC_t^{reuse}	Fixed cost of reuse unit at time period *t*
$UTC_t^{well\_storage}$	Unit transport cost from fracturing well to interim storage unit
$UTC_t^{storage\_treatment}$	Unit transport cost from interim storage unit to treatment unit
$UTC_t^{treatment\_reuse}$	Unit transport cost from treatment to reuse unit
$UTC_t^{treatment\_disposal}$	Unit transport cost from treatment to disposal unit
UP_t^{reuse}	Unit selling price of treated flowback water
$UC_t^{disposal}$	Unit disposal cost of treated flowback water
B_w	Membrane permeability
B_{wB}	Membrane properties
T_m	Average membrane temperature
$P_{w,f}^{\circ}$	Water vapor pressure of the feed
$P_{w,p}^{\circ}$	Water vapor pressure of the permeate

Variables

n_c	Number of wells
n_r	Number of fractures per well
x_f	Fracture half-length
J	Productivity of a section
k	reservoir permeability
μ_{oil}	Oil viscosity
J_{Df}	Dimensionless productivity index
A_r	Aspect ratio of a subsection
I_x	Penetration ratio of a subsection
h_{eq}	Proppant bank equilibrium height
$W_{avg,target}$	Desired average fracture width at the end of pumping
$M_{prop,frac}$	Amount of proppant injected into a single fracture
$\widehat{W}\left(t_f\right)$	Predicted average fracture width

$\widehat{W_0}(t_k)$	Fracture width at the wellbore at each sampling time t_k
$\widehat{L_0}(t_k)$	Fracture length at the wellbore at each sampling time t_k
$C_{stage,k}$	Inlet proppant concentration injected at each sampling time t_k
$Q_{stage,k}$	Inlet fracturing fluid flowrate at each sampling time t_k
${y_t}^{FB^{well\_out}}$	Flowback water recovery coefficient in time period t
FB^{well_out}	Volume constraint for the input of the flowback water model
$F_t^{storage\_in}$	Flowrate entering the interim storage unit at time period t
$F_t^{storage\_out}$	Flowrate leaving the interim storage unit at time period t
$F_t^{treatment\_in}$	Flowrate entering the treatment unit at time period t
$F_t^{treatment\_out}$	Flowrate leaving the treatment unit at time period t
$C_t^{storage\_in}$	TDS concentration entering the interim storage unit at time period t
$C_t^{storage\_out}$	TDS concentration leaving the interim storage unit at time period t
$C_t^{treatment\_in}$	TDS concentration entering the treatment unit at time period t
$C_t^{treatment\_reuse}$	TDS concentration entering reuse unit at time period t
$C_t^{treatment\_disposal}$	TDS concentration entering disposal unit at time period t
$M_t^{storage\_in}$	Mass flow of TDS concentration entering the interim storage unit
$M_t^{treatment\_in}$	Mass of TDS concentration entering the treatment unit
$M_t^{treatment\_out}$	Mass of TDS concentration leaving the treatment unit
$ff_t^{well\_storage}$	Segregated flow rate leaving from the fracturing to the interim storage unit
$ff_t^{storage\_treatment}$	Segregated flow rate leaving the interim storage unit to the treatment unit
$ff_t^{treatment\_reuse}$	Segregated flow rate leaving treatment for the reuse
$ff_t^{treatment\_disposal}$	Segregated flow rate leaving treatment for disposal
$ff_t^{treatment\_reuse}$	Segregated flow rate leaving treatment for reuse
$ff_t^{treatment\_disposal}$	Segregated flow rate leaving treatment for disposal
$mm_t^{well\_storage}$	Mass flowrate leaving from the fracturing well to the interim storage unit
$mm_t^{storage\_treatment}$	Mass flowrate leaving from the interim storage unit to the treatment unit
$mm_t^{treatment\_reuse}$	Mass flowrate leaving treatment for reuse
$mm_t^{treatment\_disposal}$	Mass flowrate leaving treatment for disposal
$ff_t^{treatment\_reuse}$	Segregated flowrate leaving treatment for reuse
$ff_t^{treatment\_disposal}$	Segregated flowrate leaving treatment for disposal

$V_t^{storage}$	Volume balance in the interim storage unit
ζ_t	Water recovery
υ_t	Recycle ratio
$J_{w,t}$	Permeate flux
$\gamma_{wf,t}$	Activity coefficient
$X_{NaCl,t}$	Mole fraction of NaCl in flowback water
$A_{m,t}$	Membrane area
$V_t^{capacity\_storage}$	Capacity for interim storage unit
$V_t^{capacity\_reuse}$	Capacity for reuse unit
$V_t^{capacity\_disposal}$	Capacity for disposal unit
$Cost_t^{disposal}$	Cost of disposal
$TC_t^{well\_storage}$	Transportation cost from fracturing well to interim storage unit
$TC_t^{storage\_treatment}$	Transportation cost from interim storage unit to treatment unit
$TC_t^{treatment\_disposal}$	Transportation cost from treatment unit to disposal site
$TC_t^{treatment\_reuse}$	Transportation cost from treatment unit to reuse water site
$CapCost_t^{storage}$	Capital cost of interim storage unit
$CapCost_t^{reuse}$	Capital cost of reuse unit
$CapCost_t^{disposal}$	Capital cost of disposal unit
$CapCost_t^{treatment}$	Capital cost of treatment unit
$WR_{prop,frac}$	Total amount of water injected to a single fracture
TAC_t	Total annual cost at time period *t*
TOC_t	Total operating cost at time period *t*
TCC	Total capital cost
$Profit^{reuse}$	Profits from selling treated flowback water at time period *t*

TABLE OF CONTENTS

Page

LIST OF FIGURES

LIST OF TABLES

Page

1. INTRODUCTION

Over the last several decades, the exploration of shale oil and gas in the Marcellus, Barnett, Fayetteville, Haynesville, and Woodford plays has allowed the United States to gradually become energy independent. Shale formation is characterized as an unconventional reservoir, because it is a self-sourced rock, implying that the reservoir (accumulated rock) is the same as the source rock. Unlike conventional reservoir where natural-oil and gas resources are found in highly permeable reservoirs, shale formation is characterized by very low absolute and effective permeability values. The low permeability of the rock formation restricts the oil and gas to easily flow to the wellbore (Zhiltsov and Shemenov, 2016). Recently, advances in technologies such as directional drilling and hydraulic fracturing have made it economically viable for oil and gas companies to produce prolific quantities of shale oil and gas (Wang and Krupnick, 2013).

In practice, the hydraulic fracturing process enhances the reservoir productivity (capacity and mobility) of low permeability reservoirs, such as tight gas and shale gas. As illustrated in **Figure 1**, the hydraulic fracturing process for well stimulation is divided into three stages. The first stage is the perforation stage, during which initial fracture paths are created along the well. Then, a hydraulic fracturing fluid is pumped at a high pressure (high enough to overcome the compressive stress of the rock), where it further propagates the fracture in the rock formation. The fracturing fluid typically consists of water, chemical additives, and proppant (quartz sand, sillica). Pumping is stopped during the closure stage, and some of the water will leak into the formation.

Furthermore, since the permeability of the proppant is high compared to the formation, the proppant-filled fractures create pathways through which oil and natural gas can easily travel from the reservoir to the wellbore. While the proppants open the fractures and prevent them from closing once the hydraulic pressure decreases, the chemical additives limit the sloughing of the shales and mud swelling, bacterial growth, corrosion, and friction (FracFocus, 2012). Moreover, achieving uniformity of proppant bank height and suspended proppant concentration across the fracture at the end of pumping determines the efficiency of the hydraulic fracturing process and the productivity of unconventional reservoirs (Siddhamshetty et al., 2018).

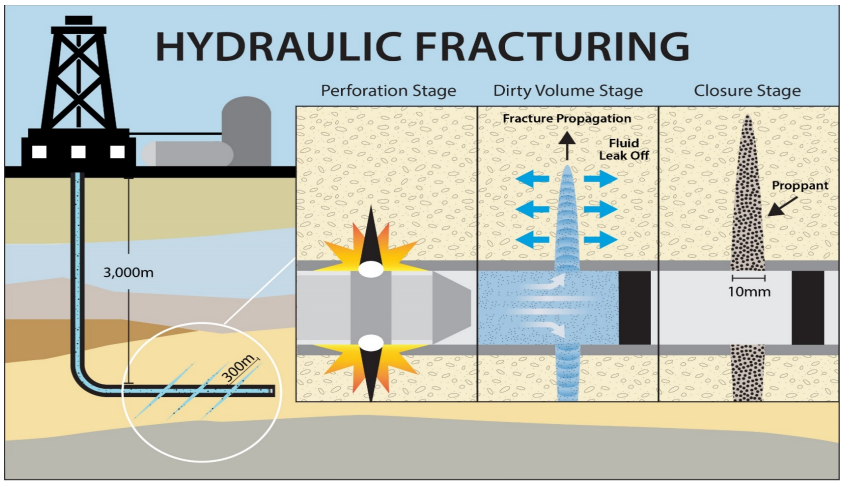

Figure 1. Schematic Illustration of Hydraulic Fracturing Operation (Reprinted from Siddhamshetty et al., 2018)

1.1 Hydraulic Fracturing Water Cycle

In the United States, the shale development continues to increase, leading to numerous concerns with respect to water consumption and management. Although the hydraulic fracturing process enhances the recovery of hydrocarbons in unconventional reservoirs, it is heavily dependent on water resources. In the five largest shale oil and gas reserves in the United States, the average water usage per well ranges from 71,000-155,000 BBL (Henderson et al., 2011; Lira-Barragan et al., 2015). The amount of water required to complete each well depends on the geological location, the characteristics of the rock formation, fracture geometry, and most importantly, the type of well (Henderson et al., 2011; Zuppann et al., 2014). Unlike horizontal wells, vertical wells tend to use less water for hydraulic fracturing operations. On average, vertical wells require 11,000-90,000 BBL for well completion, while horizontal wells require 70,000-190,000 BBL (Bai et al., 2013).

As shown in **Figure 2**, the water cycle in the hydraulic fracturing process involves five stages: water acquisition, chemical mixing, well injection, flowback and produced water, and wastewater treatment and waste disposal (US Environmental Protection Agency, 2016). In terms of water management, the stages four and five are extremely important. In Petroleum Engineering, the wastewater generated during the hydraulic fracturing process is referred to as flowback and produced water. Flowback water is defined as the fluid that contains water, dirt, sand, chemicals etc., which is recovered within the first 3-4 weeks after the hydraulic fracturing process is

completed. The amount of flowback water collected is typically 15-40% of the total injected fracturing fluid. On the other hand, the fluid known as produced water, remains in the rock formation (within the crevices and the interstitial pore spaces), and is recovered during the oil and gas production phase (Elsayed et al., 2015).

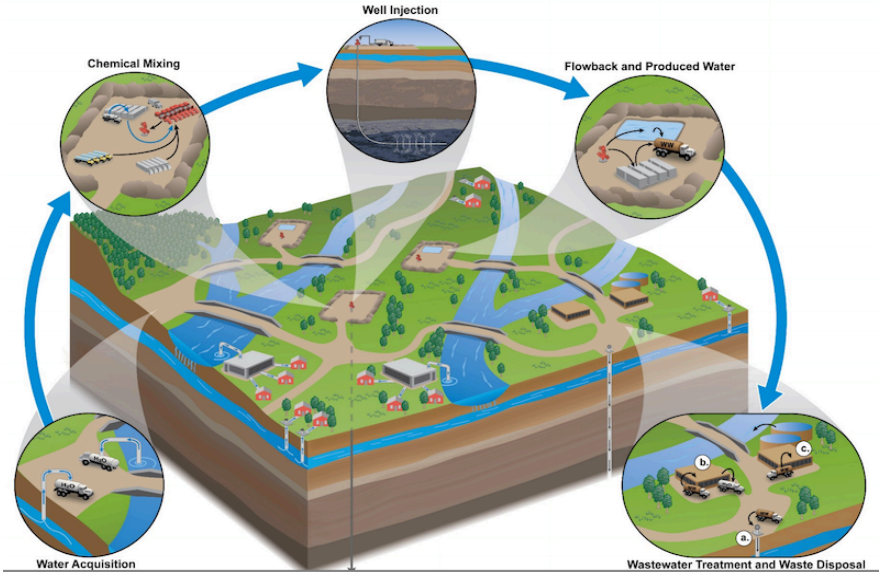

Figure 2. Hydraulic Fracturing Water Cycle
(Reprinted from US Environmental Protection Agency, 2016)

1.2 Wastewater Composition

The treatment and reuse of flowback water are viable solutions to minimize fresh water usage in hydraulic fracturing processes and negative impacts on the environment. Flowback water mostly consists of total dissolved solids (TDS) and other components such as total suspended solids (TSS), naturally occurring radioactive materials (NORM), and other elements [(US Environmental Protection Agency, 2016; Health Canada, 1991; Rosemblum et al., 2017). As the fracturing fluid resides downhole, it picks up inorganic constituents (Hayes, 2009). Consequently, the TDS concentration of the initial flowback water is low and increases over time. Flowback water with lower concentrations of TDS can be reintroduced as a fracturing fluid, whereas high-TDS flowback water has to undergo further treatment processes as it can corrode/damage drilling and downhole equipment and affect the performance of fracturing fluids (Elsayed et al. 2015).

1.3 Wastewater Management

As shown in **Figure 2**, the final stage of the hydraulic fracturing water cycle is wastewater treatment and waste disposal. The treatment strategy for the removal of TDS in wastewater depends on the several factors: the technology used, the extension of TDS removal, and fixed and operating costs (Elsayed et al. 2013; NSF; Water Research Center, 2014). While numerous efforts have been made to develop cost-effective technologies to optimize water management in hydraulic fracturing processes, the use of membrane processes as a treatment strategy has significantly increased, with an annual growth of 15% (Pangarkar et al., 2011).

Thermal membrane distillation (TMD) is a technology that uses vapor compression for wastewater treatment. The TMD system consists of the following processes and units: (i) pretreated flowback water is preheated below a boiling temperature, (ii) hydrophobic membrane, (iii) heat transfer from agent to the feed and across the membrane, and (iv) mass transfer of the water vapor (Elsayed et al. 2015). The use of TMD for treatment of flowback water in shale gas formations is a beneficial method because it has the ability to desalinate wastewater brines with high TDS concentrations and adjust capacities. Moreover, deep well injection has been the primary means for wastewater disposal. However, in some areas where shale oil and gas production is abundant, this practice is either unavailable or restricted due to indications of seismic activity because of the higher injection pressure (Water Technology, 2016). Consequently, the development of environmentally sustainable and economically feasible water management and treatment options is critical.

2. RESEARCH PROBLEM DESCRIPTION

2.1 Water Management under Uncertainty

Uncertainty is an important aspect to consider for optimal design and planning of water management in hydraulic fracturing processes. Numerous approaches and methodologies have been formulated for the synthesis of water networks in order to reduce annualized cost and environmental impact (Islam et al., 2014; Khor et al., 2014; Nápoles-Rivera et al., 2015). In this regard, understanding the life cycle of water consumption associated with shale oil and gas production is imperative for optimal water management (Jiang et al., 2014; Clark et al., 2013). As such, the optimal water usage for well completion was determined to minimize costs related to the post-fracturing process and at the same time maximize profits from gas production (Yang et al., 2014). Moreover, a shale gas supply chain network was developed to optimize the economic performance while accounting for various uncertainties related to design and operational decisions (Gao and You, 2015a; Gao and You, 2015b).

Lira-Barragan et al. (2015) has expanded optimal water management to include uncertainty in the system. In their study, uncertainties related to the amount of water required to complete each well and the flowback water collected over time are considered. A mixed-integer linear programming (MILP) problem was formulated to minimize total annual costs, which consists of capital costs (investment costs associated with the purchase of treatment, storage, and disposal units) and operating costs (fresh water costs and costs for treatment units/transportation). Nevertheless, none of the approaches mentioned above have considered hydraulic fracturing as a dynamic process whose final geometry as well as proppant bank inside the fracture has to be regulated at the end of pumping by manipulating the flow rate and concentration profiles of fracturing fluids to maximize the productivity and performance of stimulated wells.

2.2 Feedback Control for Enhanced Productivity in Shale Formations

Recently, several efforts have been made in improving the well performance via the regulation of the uniformity of proppant bank heights and suspended proppant concentration inside the fracture via real-time model-based feedback control of hydraulic fracturing (Economides et al., 2002; Gu and Hoo, 2014; Narasingam et al., 2017a; Narasingam et al., 2017b; Narasingam et al.,

2018; Siddhamshetty et al., 2017; Siddhamshetty et al., 2018; Sidhu et al., 2018; Yang et al., 2017). Specifically, the section-based optimization method developed by Liu and Valko (2017) was used to compute the optimal number of wells, number of fractures per well, half-length of the fracture that will maximize the productivity of the well-fracture system for a given total amount of proppant to be injected. Then, a model predictive control (MPC) system was developed by Siddhamshetty et al. (2018) to obtain a combination of flowrate and proppant concentration over a period of time that will achieve the desired average fracture width leading to uniform proppant bank height over the optimal fracture length at the end of pumping.

2.3 Research Motivation and Objectives

The conservation of fresh water is the overarching motivation behind the development of wastewater treatment technologies for hydraulic fracturing. The optimal flow rate of fracturing fluids, the optimal number of horizontal wells and fractures per well, the length of the fracture, and the drainage area aspect ratio that maximize the overall productivity of the well-fracture system were calculated in the approach described in Ref. [4]. However, it is important to note that the obtained pumping schedule does not consider the environmental and economic impacts of the post-fracturing process such as treatment, reuse, and disposal of flowback water. Motivated by this observation, the focus of this paper is to integrate sustainability considerations of the post-fracturing process into the hydraulic fracturing process.

In this regard, a dynamic model is developed to describe the flowrate and TDS concentration in flowback water from fractured wells, provided that the amount of water injected into the fracture well is known. Then, a thermal membrane distillation (TMD) system is considered for the removal of TDS. A multi-objective problem is formulated to optimize the entire superstructure that consists of hydraulic fracturing, storage, transportation, and water treatment, minimizing annualized cost from recovered water per period and the water footprint of the process. The capabilities of the proposed approach are illustrated through different scenarios. Furthermore, the minimum amount of water has been identified that is necessary to achieve the desired fracture length, which will not lower the productivity of the produced well.

3. METHODOLOGY AND MODELING

3.1 Schematic Diagram of the Water Management in Hydraulic Fracturing Process

In this section, a schematic diagram is constructed to present a holistic view of the water management in the hydraulic fracturing process. As shown in **Figure 3**, the flowback water management process is divided into two blocks. During the hydraulic fracturing process, a model-based feedback controller is used to determine the amount of fresh water required to inject the given amount of proppant and to achieve a uniform proppant bank height across the fracture at the end of pumping. Then, an input-output model is used to find the flowback water flowrate and TDS concentration from the well over a period of 14 days. The treatment of post-fracturing flowback water is considered using a thermal membrane distillation (TMD) for the removal of TDS. The ultimate goal is to minimize fresh water usage in the hydraulic fracturing treatment process and the total annual cost associated with the post-fracturing process.

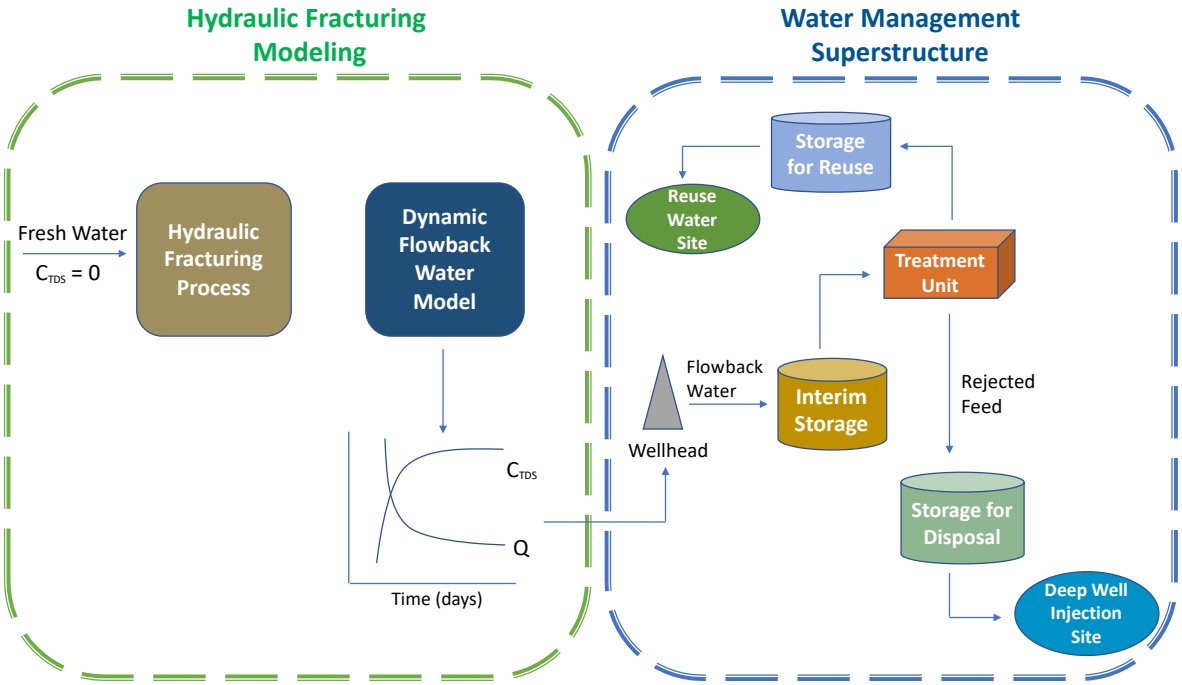

Figure 3. Proposed Diagram for the Water Management in Hydraulic Fracturing Process

3.2 Modeling and Controller Design of Hydraulic Fracturing

3.2.1 Section-based Optimization Method

Section-based optimization method is an offline optimization-based technique that was proposed by Liu and Valko (2017). This method optimizes the number of wells n_c, number of fractures per well n_r, and fracture half-length x_f, that maximizes the productivity of a stimulated well subject to a fixed amount of fracturing resources (Siddhamshetty et al., 2018). As illustrated in **Figure 4**, the section-based optimization is performed for planning a large square drainage area, which is called a section, with multi-stage fractured horizontal wells.

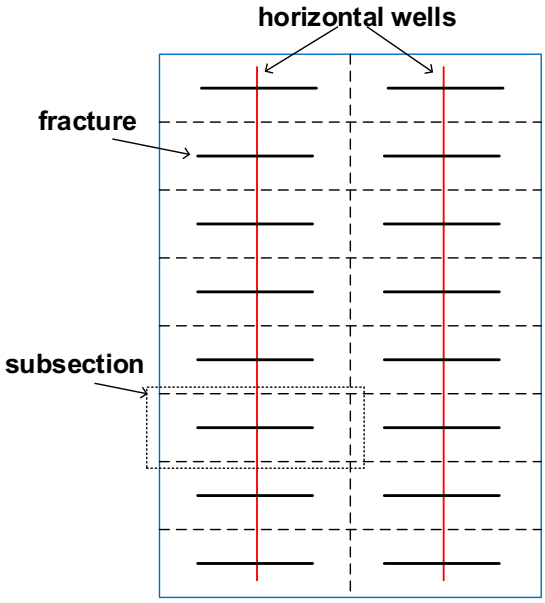

Figure 4. Illustration of a Section for the Case of Two Wells and Eight Fractures Per Well (Reprinted from Siddhamshetty et al., 2018)

The section is evenly divided into multiple subsections such that there are n_c wells and n_r fractures per well, and the drainage area stimulated by a single fracture is called a subsection. The productivity of a section with constant values for reservoir fluid properties is expressed as follows:

$$J = \frac{2\pi kH}{B\mu_{oil}} n_f J_{Df}\,(A_r, I_x) \tag{1}$$

where B is the ratio of the volume factor, which is the ratio of the volume factor of oil and gas at reservoir in-situ conditions to that at the standard condition, k is the reservoir permeability, μ_{oil} is the oil viscosity, $n_f = n_c n_r$ is the total number of fractures in the section, and J_{Df} is the dimensionless productivity index (PI) for each fracture (i.e., a subsection), which is a function of aspect ratio, $A_r = x_e/y_e$, and penetration ratio, $I_x = x_f/x_e$, of a subsection, where x_e and y_e are the half-width and half-length of the subsection, respectively (Siddhamshetty et al., 2018).

3.2.2 Optimal Well-Fracture Configuration Using Section-Based Optimization Method

In this work, the total amount of proppant for the section is $M_{prop} = 3.96\ x\ 10^7 kg$. Using the section-based optimization method, the optimal decision variables which will maximize the productivity of a section, are found to be: $n_c = 6$, $n_r = 55$, $x_f = 120\ m$, $I_x = 0.895$.

Figure 5 illustrates the growth and propagation of proppant bank height during the hydraulic fracturing process. In unconventional reservoirs, in order to create long and narrow fractures, slick water (low viscosity fluid) is predominantly used, which allows the proppant to quickly settle at the bottom of the fracture to form a proppant bank. Once the proppant bank has grown to equilibrium height, h_{eq}, the injected proppant will travel farther to find the next available location for proppant settling (Siddhamshetty et al., 2018).

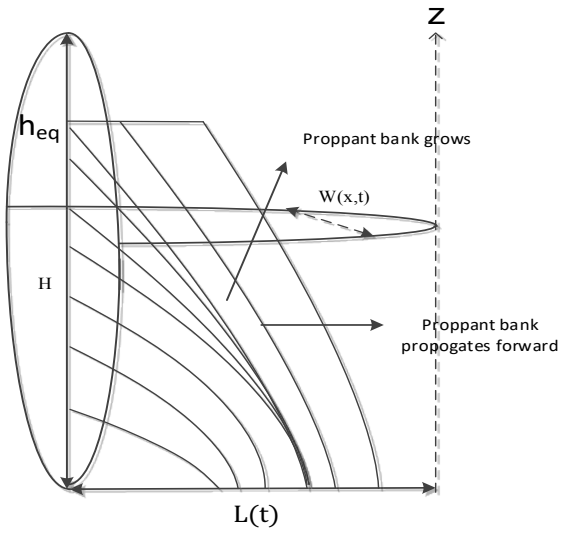

Figure 5. Growth and Propagation of Proppant Bank During a Hydraulic Fracturing Process (Reprinted from Siddhamshetty et al., 2018)

The ultimate goal is to achieve a uniform proppant bank with the equilibrium height over the optimal fracture half-length, $x_f = 120\,m$, obtained using the section-based optimization method. Assuming that the proppant bank with equilibrium height, h_{eq}, expands along the fracture to cover the entire optimal fracture half-length, x_f, the above-mentioned goal can be translated into achieving the desired average fracture width, $W_{avg,target}$, at the end of pumping, which is obtained using the following equation:

$$W_{avg,target} = \frac{M_{prop,frac}}{2\rho_p h_{eq} x_f (1-\phi)} \tag{2}$$

where the amount of proppant injected into each fracture is $M_{prop,frac} = 72{,}000\,kg$, and the equilibrium height is $h_{eq} = 54\,m$. Therefore, the calculated average fracture width at the end of pumping is, $W_{avg,target} = 5.37\,mm$ ((Siddhamshetty et al., 2018). The other values used for the simulation are illustrated in **Table 1.**

3.2.3 MPC Formulation

To achieve the desired average fracture width over the optimal fracture half-length at the end of pumping, a MPC was developed by Siddhamshetty et al. (2018). The MPC computes the optimal pumping schedule, which consists of the flowrate and proppant concentration of the fracturing fluids at the wellbore. The controller minimizes the squared deviation of the predicted average fracture width from the desired set-point value at the end of pumping, $W_{avg,target}$. In this regard, the MPC formulation is in the following form:

$$\min_{\substack{C_{stage,k\ldots,}C_{stage,9} \\ Q_{stage,k\ldots,}Q_{stage,9}}} \quad \left(\widehat{W}\left(t_f\right) - W_{avg,target}\right)^2 \tag{3}$$

$$s.t. \qquad Kalman\ filter \tag{4}$$

$$\widehat{W_0}(t_k) = W_0(t_k), \qquad \widehat{L_0}(t_k) = L_0(t_k) \tag{5}$$

$$C_{stage,k-1+m} \le C_{stage,k+m} \le 2\ PPGA \tag{6}$$

$$Q_{min} \le Q_{stage,k+m} \le Q_{max} \tag{7}$$

$$m = 1, \ldots 9-k \tag{8}$$

$$\Delta\left(\sum_{k=1}^{9} 2\, Q_{stage,k} C_{stage,k}\right) = M_{prop,frac} \tag{9}$$

In this optimization problem, Eq. (5) describes the real-time measurement of the fracture width at the wellbore $\left(\widehat{W_0}(t_k)\right)$ and fracture length $\left(\widehat{L_0}(t_k)\right)$, at each of the sampling times, t_k, which are used in the Kalman filter to estimate the average fracture width. The formulated problem also has a series of constraints. As shown by Eqs. (6) and (7), there are limits on the maximum proppant concentration injected, 2 PPGA (pounds of proppant added to one gallon of fluid), and on the flowrate of the fracturing fluids at the wellbore, Q_{max}. For in depth explanation and modeling of the section-based method and the model predictive control, the readers may refer to (Siddhamshetty et al., 2018).

Table 1. Model Parameters Used for the Simulation
(Reprinted from Siddhamshetty et al., 2018)

Parameter	Symbol	Value
Reservoir height	H	60 m
Fracturing fluid viscosity	μ	0.005 Pa · s
Proppant bank porosity during hydraulic fracturing	∅	0.61
Square drainage area of a section	A_s	2.59 x 10^6 m^2

3.3 Modeling of Flowback Water

3.3.1 Flowback Water Field Data

An input-output model is developed to predict the flowback water volumes and TDS concentration collected over the first 14 days after well completion. The data used in this model is taken from information provided by Hayes (2009). This report samples and analyzes the influent and flowback water streams at day 0, 1, 5, 14, and 90, associated with shale development of 19 locations in Pennsylvania and West Virginia (Marcellus Shale Region). As shown in **Tables 2** and **3**, the report includes the locations, types of wells, the total fracturing fluid volumes used, the associated flowback water volumes collected, and TDS concentration after well completion.

Table 2. Water Use and Flowback Water Collection Associated with Hydraulic Fracturing Completion of Shale Gas Wells (Reprinted from Hayes 2009)

Location	Well Type	Total Vol. Frac. Fluid Used, BBL	Cumulative Volume of Flowback Water, BBL			
			1 Day	5 Days	14 Days	90 Days
A	Vertical	40,046	3,950	10,456	15,023	
D	Horizontal	21,144	2,854	8,077	9,938	11,185
E	Horizontal	53,500	8,560	20,330	24,610	25,680
F	Horizontal	77,995	3,272	10,830	12,331	17,413
K	Horizontal	70,774	5,751	8,016	9,473	
M	Horizontal	99,195	16,419	17,935	19,723	
N	Vertical	11,435	2,432	2,759	3,043	3,535
Q	Vertical	23,593	1,315	3,577	5,090	
S	Vertical	16,460	2,094	7,832	9,345	

Typically in shale oil and gas development, the flowback water flowrate is initially high (2,500 to 6,000 BBL/day) and decreases over time to levels as low as 5 to 100 BBL/day (Henderson et al., 2011). On the other hand, the initial streams contain moderate to low salinity and the TDS levels gradually increase over time, reaching as high as 345,000 mg/L (Hayes, 2009). This is because the fracturing fluid injected picks up soluble inorganic constituents from the rock formation. Thus, the longer the fracturing fluid resides downhole, the higher the TDS concentration of the flowback water becomes.

Table 3. Concentration of Total Dissolved Solids in Flowback Water, mg/L (Reprinted from Hayes 2009)

Location	Day 0	Day 1	Day 5	Day 14	Day 90
A	990	15,400	54,800	105,000	216,000
B	27,800	22,400	87,800	112,000	194,000
C	719	24,700	61,900	110,000	267,000
E	5,910	28,900	55,100	124,000	
F	462	61,200	116,000	157,000	
G	1,920	74,600	125,000	169,000	
H	7,080	19,200	150,000	206,000	345,000
L	221	20,400	72,700	109,000	
O	2,670	17,400	125,000	186,000	
P	401	11,600	78,600	63,900	

3.3.2 Assumptions

To effectively develop the dynamic input-output model, the following assumptions are made:

- The total fracturing fluid volume to be injected during the hydraulic fracturing process is known.
- The flowback water recovered over the time period of 14 days is mainly from the accumulated water inside the fractures at the end of pumping.
- The TDS concentration in the flowback water will be estimated by the average of the available data provided by Hayes (2009).

3.3.3 Flowback Water Volume Model

The flowback water data from **Table 2** are correlated using a regression technique. To properly fit the data into a single function, it is normalized to facilitate comparison of the vertical and horizontal wells at each location. The following equation describes the average daily percent of fracturing water collected from the fractured well, $\left(y^{FB^{well\_out}}\right)$:

$$y^{FB^{well\_out}} = (1.254 * 10^{-6})t^6 - (6.403 * 10^{-5})t^5 + 1.306 * 10^{-3})t^4 - 0.0136t^3 + 0.076t^2 - 0.219t + 0.280 \quad (10)$$

where t is in days after well completion. The trend in **Figure 6** is as expected; the percent collected is initially high, and then it decreases over the next 14 days. The volume constraint for the input, FB^{well_out}, based on the data used to generate the model is:

$$11435\ BBL \leq FB^{well\_out} \leq 99195\ BBL \quad (11)$$

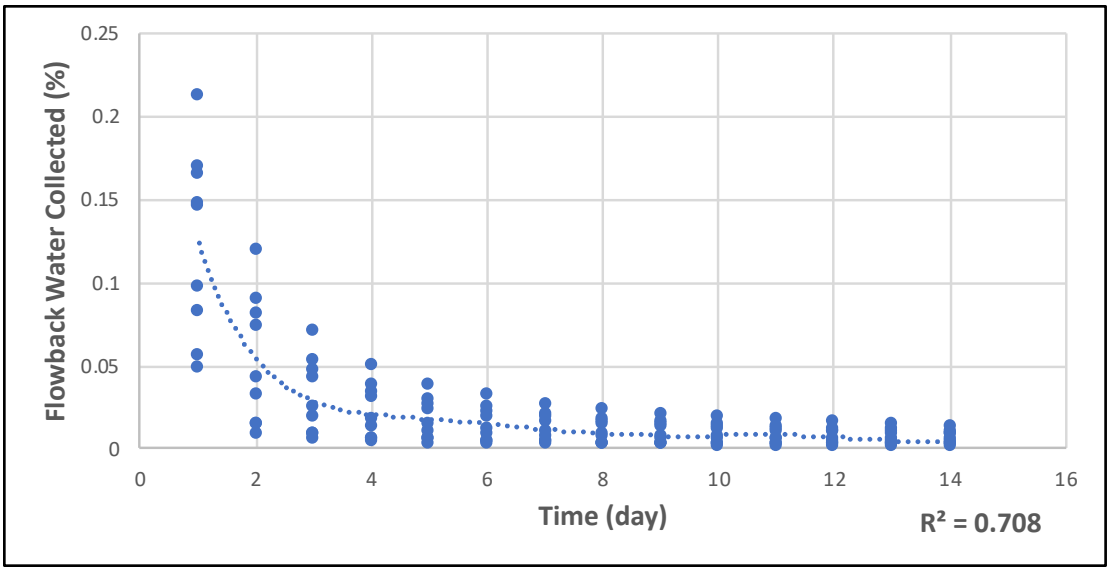

Figure 6. Flowback Water Percent Collected Regression Model

As discussed, pumping is stopped during the closure stage and some of the fracturing fluid leaks off into the formation. The pressure from the rock formation enables water along with hydrocarbons to flow from the reservoir to the wellbore. During the initial flowback phase, only the water emerges to the surface because it is within and close to the fracture. As such, the flowback water recovered is mainly from accumulated water inside the fracture at the end of pumping. Multiplying the calculated input (67,832 BBL) by $y^{FB^{well\_out}}$ obtained from the regression model, generates the outputs over the time period of 14 days. As shown in **Table 4,** the volume collected is initially 8,421 BBL on day 1, and then it decreases to as low as 205 BBL on day 14.

Table 4. Flowback Water Volume Collected Based on Regression Model

Day	Average Flowback Recovery Coefficient (%)	Flowback Water Volume (BBL)
1	12.4	8,421
2	5.45	3,705
3	2.86	1,943
4	2.07	1,405
5	1.78	1,210
6	1.50	1,021
7	1.18	799
8	0.90	613
9	0.78	525
10	0.77	521
11	0.76	513
12	0.59	404
13	0.29	200
14	0.30	205

3.3.4 Flowback Water TDS Concentration Model

TDS concentration is highly dependent on the rock formation; therefore it changes from one location to another. In this work, the TDS concentration in the flowback water is assumed to be the average of the available data provided by Hayes (2009). The TDS concentration profile over the time period of 14 days is fixed at the average value for each scenario, regardless of the location of the shale play, geological formation, and chemicals introduced during the drilling and hydraulic fracturing operation.

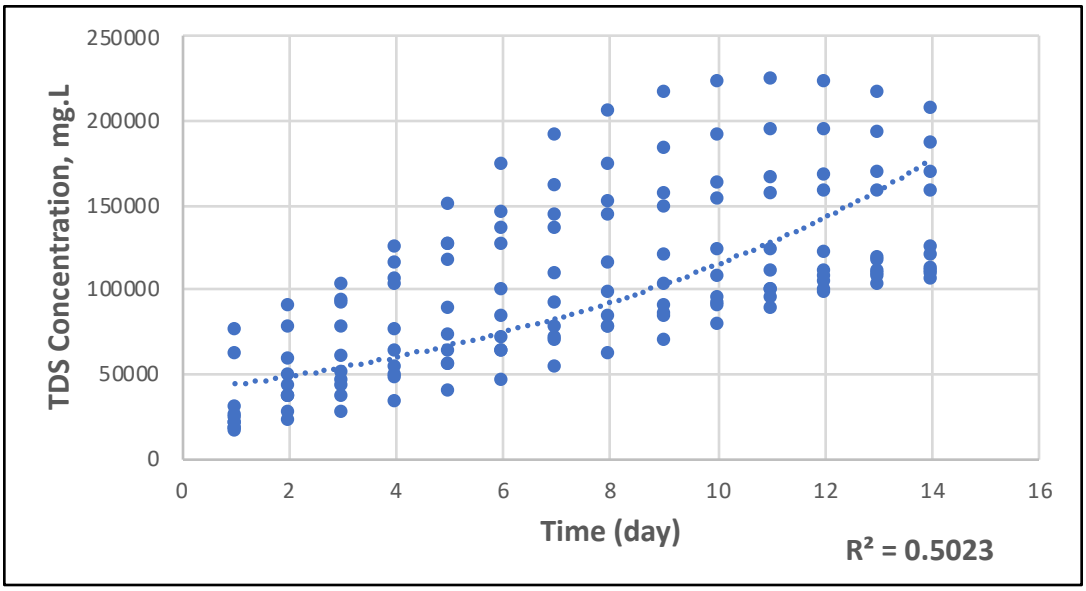

Figure 7. TDS Concentration Regression Model

An exponential regression is used to correlate the TDS concentration with time. It is shown in **Figure 7**. The longer the fracturing fluid remains downhole, the higher the TDS levels become. Fitting the data using a single function generates the following equation for the average TDS concentration of flowback water, C^{well_out}, as a function of time that comes out of the fractured well:

$$C^{well\_out} = 39092e^{0.1079t} \tag{12}$$

where t is in days from the beginning of a hydraulic fracturing event. Using Eq. (12), the predicted TDS concentration in the collected flowback water over the first 14 days is shown in **Table 5**.

Table 5. TDS Concentration in Flowback Water Based on Regression Model

Day	TDS Concentration, mg/L
1	43,546
2	48,507
3	54,034
4	60,191
5	67,049
6	74,688
7	83,198
8	92,677
9	103,236
10	114,998
11	128,101
12	142,696
13	158,954
14	177,065

3.4 Modeling of Post-Fracturing Flowback Water Treatment Process

3.4.1 Mass Balance Equations

The increasing salt concentration (TDS level) over time in flowback water is an important component of the collected stream, as it determines the disposal options, treatment strategies, and most importantly, treatment cost. To properly develop and implement the proposed methodology, mass balances for the storage unit, TMD technology, and the reuse/disposal options are considered.

3.4.1.1 Flowback Water

In this model, the main objective is to analyze the impact of flowback water attributes on the economic performance of the system, while considering environmental factors. As shown in the proposed superstructure illustrated in **Figure 3**, the flowback water collected goes through a treatment unit for TDS removal. This practice does not only avoid the disposal of untreated flowback water, it also represents environmental remediation (Lira-Barragan et al., 2015). The mass balance equations are given as follows: the outlet water $\left(F_t^{well\_out}\right)$ from the fractured well at time period t enters the interim storage $\left(ff_t^{well\_storage}\right)$:

$$F_t^{well\_out} = ff_t^{well\_storage}, \quad \forall t \tag{13}$$

The flowback water stream has TDS concentration associated with it. The following mass flow rate $\left(mm_t^{well\_storage}\right)$ is considered for the outlet concentration $\left(C_t^{well\_out}\right)$ into the interim storage unit:

$$mm_t^{well\_storage} = C_t^{well\_out} * ff_t^{well\_storage}, \quad \forall t \tag{14}$$

3.4.1.2 Water Inlet to Storage Unit

Flowback water that comes out of the well enters an interim storage unit before treatment. This storage unit is local, i.e. low transportation costs. The following equation describes the flowback water that enters the storage unit at time period t $\left(F_t^{storage\_in}\right)$ is same as that coming out from the well at the same time period:

$$F_t^{storage\_in} = ff_t^{well\_storage}, \quad \forall t \tag{15}$$

The mass flow of the TDS $\left(M_t^{storage\_in}\right)$ and the corresponding concentration $\left(C_t^{storage\_in}\right)$ entering the storage unit is provided by Eqs. (16) and (17), respectively:

$$M_t^{storage\_in} = mm_t^{well\_storage}, \quad \forall t \tag{16}$$

$$C_t^{storage\_in} = \frac{M_t^{storage\_in}}{F_t^{treatment\_in}}, \quad \forall t \tag{17}$$

3.4.1.3 Water Outlet from Storage Unit

The flowback water from the storage unit is transported to the separation technology (TMD system) for regeneration and disposal of rejected feed at time period t $\left(ff_t^{storage\_treatment}\right)$. The equations for the outlet flow $\left(F_t^{storage\_out}\right)$ and mass flow of TDS from the storage unit $\left(mm_t^{storage\_treatment}\right)$ are as follows:

$$F_t^{storage\_out} = ff_t^{storage\_treatment}, \quad \forall t \tag{18}$$

$$mm_t^{storage\_treatment} = C_t^{storage\_out} * ff_t^{storage\_treatment}, \quad \forall t \tag{19}$$

3.4.1.4 Water Inlet for Treatment

In this study, a thermal membrane distillation system is considered to treat the wastewater brines (flowback water). This technology efficiently treats wastewater under adequate conditions to be disposed or reused, while minimizing cost and environmental impacts (Lira-Barragan et al., 2015). Compared to reverse osmosis, thermal membrane processes are more suitable for the recovery and desalination of high-TDS flowback water (Pangarkar et al., 2011). The flowback water entering the treatment technology at time period *t* ($F_t^{treatment\_in}$) is supplied by the outlet streams from the storage unit ($ff_t^{storage\_treatment}$):

$$F_t^{treatment\_in} = ff_t^{storage\_treatment}, \quad \forall t \tag{20}$$

The mass flow of the TDS and the inlet concentration are:

$$M_t^{treatment\_in} = mm_t^{storage\_treatment}, \quad \forall t \tag{21}$$

$$C_t^{treatment\_in} = \frac{M_t^{treatment\_in}}{F_t^{treatment\_in}}, \quad \forall t \tag{22}$$

3.4.1.5 Water Outlet from Treatment Units

The present model represents an open-loop problem where the streams will not be reintroduced as a fracturing fluid to another well. Depending on the optimization scheme (parameters, variables, costs, etc.), only a portion of the flowback water will be recovered for reuse, while the rest may have to be disposed. In this regard, the outlet flowrate from the TMD system ($F_t^{treatment\_out}$) over time period *t* will be transported to a water reuse site for profits or to disposal via deep well injection*:*

$$F_t^{treatment\_out} = ff_t^{treatment\_reuse} + ff_t^{treatment\_disposal}, \quad \forall t \tag{23}$$

The mass flow of the TDS and the outlet concentration for each end purpose are illustrated by Eqs. (24) through (26):

$$M_t^{treatment\_out} = mm_t^{treatment\_reuse} + mm_t^{treatment\_disposal}, \quad \forall t \tag{24}$$

$$mm_t^{treatment\_reuse} = C_t^{treatment\_reuse} * ff_t^{treatment\_reuse}, \quad \forall t \tag{25}$$

$$mm_t^{treatment\_disposal} = C_t^{treatment\_disposal} * ff_t^{treatment\_disposal}, \quad \forall t \tag{26}$$

3.4.1.6 Volume Balances in Storage Unit

To calculate the volume balance in the storage unit over time, the previous volume in time period *t-1* (for the 14 day time period), the time conversion factor H^{time}, and the difference between the inlet and outlet flowrate are considered (Lira-Barragan et al., 2015). H^{time} is defined as the operating days per time period (86400 sec/day). As such, the volume balance in the storage unit is given by the following equations for each time period *t*:

$$V_t^{storage} = V_t^{storage\_initial} + H^{time} * \left(F_t^{storage\_in} - F_t^{storage\_out}\right), \quad \forall t = 1 \tag{27}$$

$$V_t^{storage} = V_{t-1}^{storage} + H^{time} * \left(F_t^{storage\_in} - F_t^{storage\_out}\right), \quad \forall t > 1 \tag{28}$$

$$V_t^{storage} = 0, \quad \forall t = 14 \tag{29}$$

The TDS concentration balance for each time period in the interim storage unit is provided by Eqs. (30) through (32):

$$C_t^{storage\_out} = C_t^{storage\_in}, \quad \forall t = 1 \tag{30}$$

$$C_t^{storage\_out} * \left(V_{t-1}^{storage} + H^{time} * F_t^{storage\_in}\right) = C_{t-1}^{storage\_out} * V_{t-1}^{storage} + H^{time} * F_t^{storage\_in}, \quad \forall t > 1 \tag{31}$$

$$C_t^{storage\_out} * H^{time} * F_t^{storage\_in} = C_{t-1}^{storage\_out} * V_{t-1}^{storage} + C_t^{storage\_in} * H^{time} * F_t^{storage\_in}, \quad \forall t = 14 \tag{32}$$

3.4.2 Thermal Membrane Distillation Design

The TMD system used in this model was developed by Elsayed et al. (2013). As mentioned, TMD is a membrane technology that uses vapor compression for wastewater treatment. First, the flowback water is pretreated to remove oils, organic compounds, and bacteria. Then, the pretreated flowback water is preheated below a boiling temperature to avoid complete evaporation of the feed. Finally, the water vapor travels through the membrane and is condensed on the permeate side

by large quantities of sweeping water (clean water) (Elsayed et al., 2013; Elsayed et al., 2015). Through this process, complete TDS rejection is assumed. As such, the treated flowback water (permeate) is virtually pure water (i.e. $C_t^{treatment\_reuse} = 0$). In this regard, the water recovery (ζ_t) described in Eq. (33) is the ratio of the permeate flowrate to the flowrate fed to the TMD system:

$$\zeta_t = \frac{F_t^{treatment\_in}}{ff_t^{treatment\_reuse}}, \quad \forall\, t \tag{33}$$

To increase water recovery, a portion of the rejected stream leaving the TMD system $\left(ff_t^{treatment\_disposal}\right)$ is reheated and recycled back by mixing with the feed [15]. The following equation describes the recycle ratio (υ_t) of the recycled flowrate to the feed flowrate.

$$\upsilon_t = \frac{ff_t^{treatment\_disposal}}{F_t^{treatment\_in}}, \quad \forall\, t \tag{34}$$

Furthermore, the permeate flux ($J_{w,t}$) is one of the key equations in this model. As shown in Eq. (35), B_w is the membrane permeability, a function of the membrane properties $\left(B_{wB} = 7.5 * 10^{-11} \frac{kg}{m^2 * s * Pa * K^{1.334}}\right)$ and the average membrane temperature, $T_m = 363\ K$. Eq. (36) describes the water vapor pressure of the feed ($P_{w,f}^{\circ}$), while Eq. (37) describes the water vapor pressure of the permeate ($P_{w,p}^{\circ}$). The activity coefficient of the water in the feed ($\gamma_{wf,t}$) is described by Eq. (38). Moreover, as shown by Eq. (39), ($X_{NaCl,t}$) is the mole fraction of NaCl of the feed. Finally, the area of the membrane $\left(A_{m,t}\right)$ described in Eq. (40) is the ratio of the permeate flowrate to the permeate flux (Elsayed et al., 2013; Elsayed et al., 2015):

$$J_{w,t} = B_w * \left(P_{w,f}^{\circ} * \gamma_{wf,t} - P_{w,p}^{\circ}\right), \quad \forall\, t \tag{35}$$

$$P_{w,f}^{\circ} = \exp\left(23.1964 - \frac{3816.44}{T_{m,f} - 46.13}\right) \tag{36}$$

$$P_{w,p}^{\circ} = \exp\left(23.1964 - \frac{3816.44}{T_{m,p} - 46.13}\right) \tag{37}$$

$$\gamma_{wf,t} = 1 - 0.5X_{NaCl,t} - 10X_{NaCl,t}^2, \quad \forall\, t \tag{38}$$

$$X_{NaCl,t} = \frac{\frac{C_t^{treatment\_in}}{58}}{\frac{C_t^{treatment\_in}}{58} + \frac{1 - C_t^{treatment\_in}}{18}}, \quad \forall\, t \tag{39}$$

$$A_{m,t} = \frac{ff_t^{treatment\_reuse}}{J_{w,t}}, \quad \forall\, t \tag{40}$$

3.4.3 Constraints

3.4.3.1 Volume Capacity

There is a maximum capacity available for the storage, reuse, and disposal units. Given the time conversion factor and the previous volume at time *t-1,* the storage volume at time *t* will increase as wastewater flows into the storage unit over time. Similarly, as the treated wastewater flows into the reuse (or disposal) unit, the associated volume capacity will increase over time. As described in the following equations, to effectively optimize the system, the maximum capacity available cannot be exceeded:

(a) Storage Capacity:

$$V_t^{capacity\_storage} \geq V_t^{storage}, \quad \forall\, t \tag{41}$$

(b) Reuse Capacity:

$$V_t^{reuse} = H^{time} * F_t^{reuse\_in}, \quad \forall\, t \tag{42}$$

$$V_t^{capacity\_reuse} \geq V_t^{reuse}, \quad \forall\, t \tag{43}$$

(c) Disposal Capacity:

$$V_t^{disposal} = H^{time} * F_t^{disposal\_in}, \quad \forall\, t \tag{44}$$

$$V_t^{capacity\_disposal} \geq V_t^{disposal}, \quad \forall\, t \tag{45}$$

3.4.3.2 TDS Constraints

As mentioned, the stream that comes out of the treatment system for reuse is virtually pure water, i.e. the TDS concentration = 0. The constraint associated with the treated wastewater is presented in the following equation:

$$C_t^{treatment\_reuse} = 0, \quad \forall\, t \tag{46}$$

Moreover, to avoid build up contaminants and precipitation in the TMD system, the TDS level in the reject should not exceed 0.35 (Elsayed et al., 2015). The maximum TDS weight fraction allowed is provided by the following equation:

$$C_t^{capacity\_disposal} \leq 0.35\,, \qquad \forall\, t \tag{47}$$

3.4.4 Objective Function

3.4.4.1 Total Annual Cost

The proposed methodology is a mixed-integer non-linear programing (MINLP) problem that was implemented in General Algebraic Modeling System (GAMS), and solved using the BARON solver. The objective is to optimize the expected total annual cost associated with the post-fracturing process. As shown by Eq. (48), the total annual cost consists of total capital cost, total operating cost, and profits from selling the treated flowback water:

$$TAC_t = TOC_t + TCC - Profit_t^{reuse}\,, \qquad \forall\, t \tag{48}$$

3.4.4.2 Total Operating Cost

In this model, the operating costs are related to all of the expenses associated with wastewater treatment, disposal, and transportation.

a) Treatment Costs

Before going through the TMD system, the generated flowback stream is pretreated to remove oils, bacteria, and organic compounds (Elsayed et al., 2015). All of the annual costs associated with the pretreatment and treatment processes are presented as follows:

$$Cost_t^{treatment} = \{[1411 + 43 * (1 - \zeta)] + [1613 * (1 + \upsilon)]\} * F_t^{treatment\_in}\,, \quad \forall\, t \tag{49}$$

b) Disposal Costs

As discussed, deep well injection has been the primary means of management for disposal of high-TDS wastewater. In this regard, the cost of disposal $\left(Cost_t^{disposal}\right)$ is the product of the unit cost of disposal $\left(UC_t^{disposal}\right)$ and the associated flowrate:

$$Cost_t^{disposal} = UC_t^{disposal} * F_t^{disposal\_in}, \quad \forall t \tag{50}$$

c) Transportation Costs

The total operating cost equation mostly consists of the transportation costs to send flowback water streams from one network to the other. In this model, the interim storage unit is onsite, thus the unit transportation cost $(UTC_t^{well\_storage})$ is relatively low. The transportation cost $(TC_t^{well\_storage})$ from the fractured well to the storage unit is provided by Eq. (51):

$$TC_t^{well\_storage} = UTC_t^{well\_storage} * ff_t^{well\_storage}, \quad \forall t \tag{51}$$

In theory, the treatment technology should be located close to the well operation site, to further minimize hauling costs. The TMD technology used in this model is a mobile system that can be moved from one well to the other, depending on the operators' demand (Elsayed et al., 2015). The transportation cost from the storage unit to the TMD system is provided by Eq. (52):

$$TC_t^{storage\_treatment} = UTC_t^{storage\_treatment} * ff_t^{storage\_treatment}, \quad \forall t \tag{52}$$

The flowback water data generated in the dynamic input-output model comes from data samples associated with shale development in the Marcellus Region. As previously mentioned, there are few injection sites in that region (Henderson et al., 2011). Consequently, the generated flowback water needs to be transported to sites in Ohio or Indiana. In this regard, the unit transportation cost $(UTC_t^{treatment\_disposal})$ of such long distances is high. The transportation cost $(TC_t^{treatment\_disposal})$ from the TMD system to the disposal unit for deep well injection is provided by Eq. (53):

$$TC_t^{treatment\_disposal} = UTC_t^{treatment\_disposal} * ff_t^{treatment\_disposal}, \quad \forall t \tag{53}$$

The transportation cost from the TMD system to reuse water sites for profit is provided by Eq. (54):

$$TC_t^{treatment\_reuse} = UTC_t^{treatment\_reuse} * ff_t^{treatment\_reuse}, \quad \forall t \tag{54}$$

d) Profits

As shown in the following equation, treated water will be transported to a reuse water site and sold for profit:

$$Profit_t^{reuse} = UP_t^{reuse} * F_t^{reuse\_in}, \quad \forall\, t \tag{55}$$

3.4.4.3 Total Capital Cost

In this model, the capital costs are related to equipment acquisition associated with wastewater storage, treatment, and disposal. Given the annualized factor $K = 0.1$, the fixed and variable costs, and the maximum volume capacity for each, the capital cost equations are presented in the following form:

$$CapCost_t^{storage} = K * \left[FC_t^{storage} + \left(VC_t^{storage} * V_t^{capacity\_storage}\right)\right], \quad \forall t \tag{56}$$

$$CapCost_t^{reuse} = K * \left[FC_t^{reuse} + \left(VC_t^{reuse} * V_t^{capacity\_reuse}\right)\right], \quad \forall\, t \tag{57}$$

$$CapCost_t^{disposal} = K * \left[FC_t^{disposal} + \left(VC_t^{disposal} * V_t^{capacity\_disposal}\right)\right], \quad \forall\, t \tag{58}$$

$$CapCost_t^{treatment} = 58 * A_{m,t} + 1115 * F_t^{treatment\_in}, \quad \forall\, t \tag{59}$$

3.4.4.4 MINLP Model

Based on the detailed mathematical model presented in the previous sections, the problem of optimal wastewater management related to the post-fracturing operations can be posed as a multi-objective MINLP problem, as follows:

$$min \quad TAC = TOC + TCC - Profit^{reuse} \tag{60}$$

$$s.t. \quad Eq.(13) - (59) \tag{61}$$

4. RESULTS AND DISCUSSION

Some of the key barriers for shale gas development are related to water availability for the hydraulic fracturing process, as well as the treatment and disposal of the water collected as flowback after well completion (Henderson et al., 2011; Jiang et al., 2014). In the Marcellus Shale Region, the average amount of water required to complete one well is roughly 92,000 BBL. Thus water availability (and scarcity) can become an issue, especially in places where there is apparent competition between water usage for energy production and agriculture, for instance. In this regard, a multi-objective optimization problem is formulated to minimize the total annual cost associated with the post-fracturing process, as well as the water footprint. The capabilities of the proposed approach are illustrated through different scenarios, and a sensitivity analysis examines the effects of water availability on the productivity of stimulated wells. Finally, the impact of wastewater generation is evaluated using the tool for reduction and assessment of chemical and other environmental impacts (TRACI).

4.1 Base Case

In the base case, the proposed MPC computes the optimal pumping schedule without any constraint on the availability of fresh water for the hydraulic fracturing operation. By assuming there is unlimited fracturing fluid available, the optimal pumping schedule will generate a uniform proppant bank height across the fracture at the end of pumping. Then, the dynamic input-output model discussed in **Section 3.3** describes the flowrate and TDS concentration in flowback water reported in **Table 6.** Finally, the flowback water data is used in the post-fracturing process to minimize TAC. **Table 7** illustrates the parameters used in the post-fracturing process optimization problem (Boschee, 2014; Collins, 2016; Elsayed et al., 2015; Henderson et al., 2011; Lira-Barragan et al., 2015).

Table 6. Flowback Water Data Based on Dynamic Input-Output Model

Day	Flowrate of Flowback (kg/s)	Mass Fraction of TDS
1	15.5	0.044
2	6.82	0.049
3	3.58	0.054
4	2.59	0.060
5	2.23	0.067
6	1.88	0.075
7	1.47	0.083
8	1.13	0.093
9	0.97	0.103
10	0.96	0.115
11	0.94	0.128
12	0.74	0.143
13	0.37	0.159
14	0.37	0.177

Table 7. Model Parameters Used in the Optimization Problem

	Treatment	Storage	Disposal	Reuse
Fixed cost, $	Refer to Eq. (59)	10,000	52,000	10,000
Variable cost, $/kg	Refer to Eq. (49)	0.0063	0.0135	0.0063
Unit transportation cost, $/kg	0.00036	0.00036	0.15	0.03
Cost of disposal, $/kg			0.04	
Selling price, $/kg				0.004

The costs associated with treatment and disposal of flowback water over the 14 day time period are reported in **Table 8**. Since the selling price per kilogram of the treated flowback water

is relatively low compared to the total cost of treatment, meaningful profit is unattainable in this problem. The only way to make profit in the post-fracturing process is by increasing the selling price and/or finding reuse and disposal sites that are closer to the hydraulic fracturing operation site. However, increasing the selling price of treated flowback water is not feasible because if it is too high, it is more cost effective to use fresh water. Furthermore, there are only few disposal sites in the Marcellus Shale region, which explains the high hauling cost of $0.15/kg. Thus finding disposal sites that are closer is also a problem due to availability. In this regard, the productivity of the stimulated well is extremely important, as it will determine how much money is made from the hydraulic fracturing operation.

Table 8. Costs and Profit Associated with Treatment and Disposal of Flowback Water

	Value
Disposal cost	$24,125
Profit from selling treated flowback water	$11,819
Treatment cost	$13,1160
Transportation cost to well	$1,230
Transportation cost to treatment unit	$1,230
Transportation cost to reuse site	$84,420
Transportation cost to disposal site	$90,467
Capital cost of storage unit	$3,133
Capital cost of treatment unit	$135,650
Capital cost of reuse unit	$2,773
Capital cost of disposal unit	$6,014

Moreover, to get a better idea of how TAC changes, the cumulative TAC and percent recovery of the flowback water is plotted for each time period. As shown in **Figure 8,** the cumulative TAC increases almost linearly throughout the post-fracturing process from $176,256 for one day of treatment and disposal to $468,379 when the process is done for all 14 days. The percent recovery reported in **Table 9** refers to the flowback water recovered from the TMD system.

As shown, more than 50% of the flowback water collected is recovered within day 3. Over the 14 day period, 82.3% of the total flowback water collected is recovered through treatment.

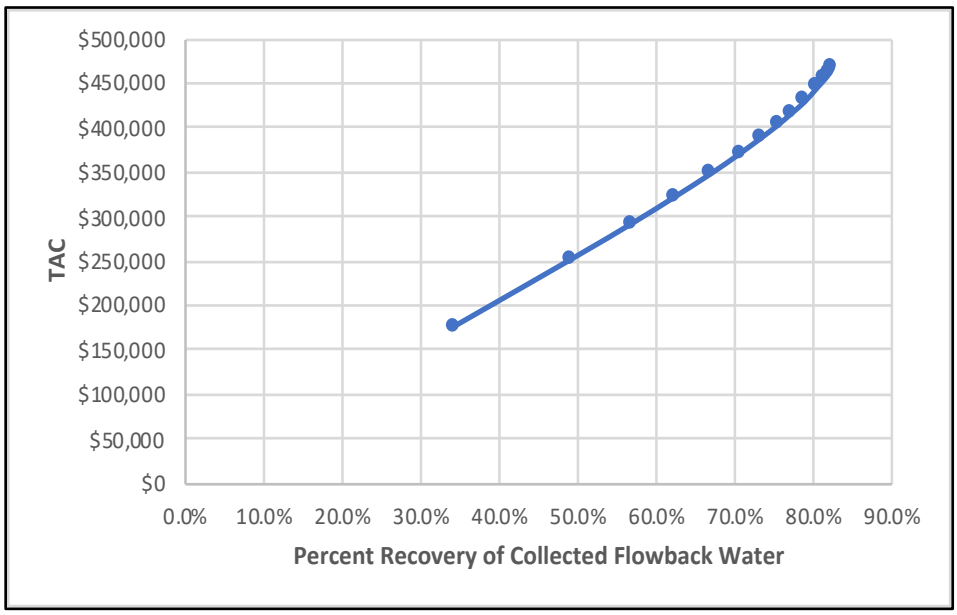

Figure 8. Cumulative TAC and Percent Recovery for the Base Case

Table 9. Cumulative TAC and Percent Recovery Values for the Base Case

Day*	Cumulative TAC	Recovery (%)
1	$176,256	34.3%
2	$251,984	49.1%
3	$292,440	56.7%
4	$322,321	62.2%
5	$348,663	66.7%
6	$371,462	70.5%
7	$389,854	73.3%
8	$404,255	75.4%
9	$417,282	77.1%
10	$430,610	78.8%
11	$445,629	80.3%
12	$456,635	81.4%
13	$462,386	81.9%
14	$468,379	82.3%

*Days from the hydraulic fracturing event.

4.2 Scenario I-IV: Reduction in Total Fracturing Fluid Injected

Compared to the base case, there is a limit on the total water available for scenarios I through IV. As such, a constraint is introduced in the proposed MPC to find the new optimal pumping schedule. In this regard, the revised MPC formulation from **Section 3.2.3** will include the following equation:

$$\Delta\left(\sum_{k=1}^{9} 2\, Q_{stage,k}\right) = WR_{prop,frac} \tag{62}$$

where $Q_{stage,k}$ is the fracturing fluids flowrate and $C_{stage,k}$ is the proppant concentration that have to be injected at each time interval to achieve uniform proppant bank height across the fracture.

Furthermore, the constraint of Eq. (62) refers to the amount of water to be injected in a single fracture over the entire hydraulic fracturing process, $WR_{prop,frac} = 241.09\, m^3$ for the base case. In this regard, the constraint for a 10% reduction in the water available (scenario I) is, $WR_{prop,frac} = 216.98\, m^3$. The results for water availability and requirements based on 20% (scenario II), 30% (scenario III), and 40% (scenario IV) reductions are tabulated in **Table 10.**

Table 10. Water Requirements Based on Volume Reduction for Scenarios I-IV

	Total Water Injected, $WR_{prop,frac}$ (m^3)
Scenario I: 10% Reduction	216.98
Scenario II: 20% Reduction	192.90
Scenario III: 30% Reduction	167.86
Scenario IV: 40% Reduction	145.11

Using the proposed MPC for the hydraulic fracturing process, provided the new constraint imposed on the amount of water to be injected, the new optimal pumping schedule for each scenario can be obtained. Then, it is applied to the high fidelity model to get the total water volume inside the fracture, which is used in the dynamic input-output model to generate the flowback water flowrate and TDS concentration reported in **Tables 11-14.** Compared to the base case, there

is a 23% reduction in the flowrate on day 1 for scenario II. Moreover, the new data is implemented in GAMS to optimize the total annual costs associated with the post-fracturing process.

Table 11. Flowback Water Data Based on Dynamic Input-Output Model for Scenario I (10% Reduction)

Day	Flowrate of Flowback (kg/s)	Mass Fraction of TDS
1	13.98	0.044
2	6.15	0.049
3	3.23	0.054
4	2.33	0.060
5	2.01	0.067
6	1.69	0.075
7	1.32	0.083
8	1.02	0.093
9	0.87	0.103
10	0.86	0.115
11	0.85	0.128
12	0.67	0.143
13	0.33	0.159
14	0.33	0.177

Table 12. Flowback Water Data Based on Dynamic Input-Output Model for Scenario II (20% Reduction)

Day	Flowrate of Flowback (kg/s)	Mass Fraction of TDS
1	11.99	0.044
2	5.28	0.049
3	2.77	0.054
4	2.00	0.060
5	1.72	0.067
6	1.45	0.075
7	1.14	0.083
8	0.87	0.093
9	0.75	0.103
10	0.74	0.115
11	0.73	0.128
12	0.57	0.143
13	0.29	0.159
14	0.29	0.177

Table 13. Flowback Water Data Based on Dynamic Input-Output Model for Scenario III (30% Reduction)

Day	Flowrate of Flowback (kg/s)	Mass Fraction of TDS
1	11.81	0.044
2	5.2	0.049
3	2.73	0.054
4	1.97	0.060
5	1.7	0.067
6	1.43	0.075
7	1.12	0.083
8	0.86	0.093
9	0.74	0.103
10	0.73	0.115
11	0.72	0.128
12	0.57	0.143
13	0.28	0.159
14	0.28	0.177

Table 14. Flowback Water Data Based on Dynamic Input-Output Model for Scenario IV (40% Reduction)

Day	Flowrate of Flowback (kg/s)	Mass Fraction of TDS
1	10.63	0.044
2	4.68	0.049
3	2.45	0.054
4	1.77	0.060
5	1.53	0.067
6	1.29	0.075
7	1.01	0.083
8	0.77	0.093
9	0.66	0.103
10	0.65	0.115
11	0.64	0.128
12	0.51	0.143
13	0.25	0.159
14	0.25	0.177

Similar to the base case, the cumulative TAC and percent water recovery are plotted for each time period. As reported in **Table 15**, the reduced volume injected does not affect the amount recovered from the TMD system. As such, there is a 56.8% and 82.3% recovery by day 3 and 14, respectively for each scenario. The flow reduction only affects the cumulative TAC of each scenario. In other words, TAC for the base case is higher than the other scenarios because the volume of injected fracturing fluid and the volume of collected flowback water are higher. In this regard, TAC for scenario III and IV after 14 days are $358,660 and $323,023 respectively. Compared to the base case, there is a 23% reduction in TAC for scenario III and a 31% reduction for scenario IV. From **Figure 9**, the cumulative TAC increases almost linearly over the 14 day period for each scenario.

Table 15. Cumulative TAC and Percent Recovery Values for Scenarios I-IV

Day*	Recovery (%)	Scenario I	Scenario II	Scenario III	Scenario IV
1	**34.3%**	$159,678	$137,973	$136,010	$123,140
2	**49.1%**	$227,966	$196,601	$193,750	$175,106
3	**56.8%**	$264,467	$227,904	$224,600	$202,792
4	**62.2%**	$291,348	$250,978	$247,328	$223,213
5	**66.7%**	$315,091	$271,295	$267,409	$242,349
6	**70.5%**	$335,586	$288,880	$284,751	$258,077
7	**73.3%**	$353,611	$304,437	$298,686	$270,724
8	**75.4%**	$366,776	$315,567	$311,140	$280,653
9	**77.1%**	$378,342	$325,637	$320,977	$289,427
10	**78.7%**	$390,173	$335,817	$331,020	$298,369
11	**80.3%**	$402,302	$346,234	$341,294	$307,502
12	**81.4%**	$412,267	$354,712	$349,772	$315,087
13	**81.9%**	$417,397	$359,219	$354,125	$318,973
14	**82.3%**	$422,742	$359,228	$358,660	$323,023

***Days from the hydraulic fracturing event.

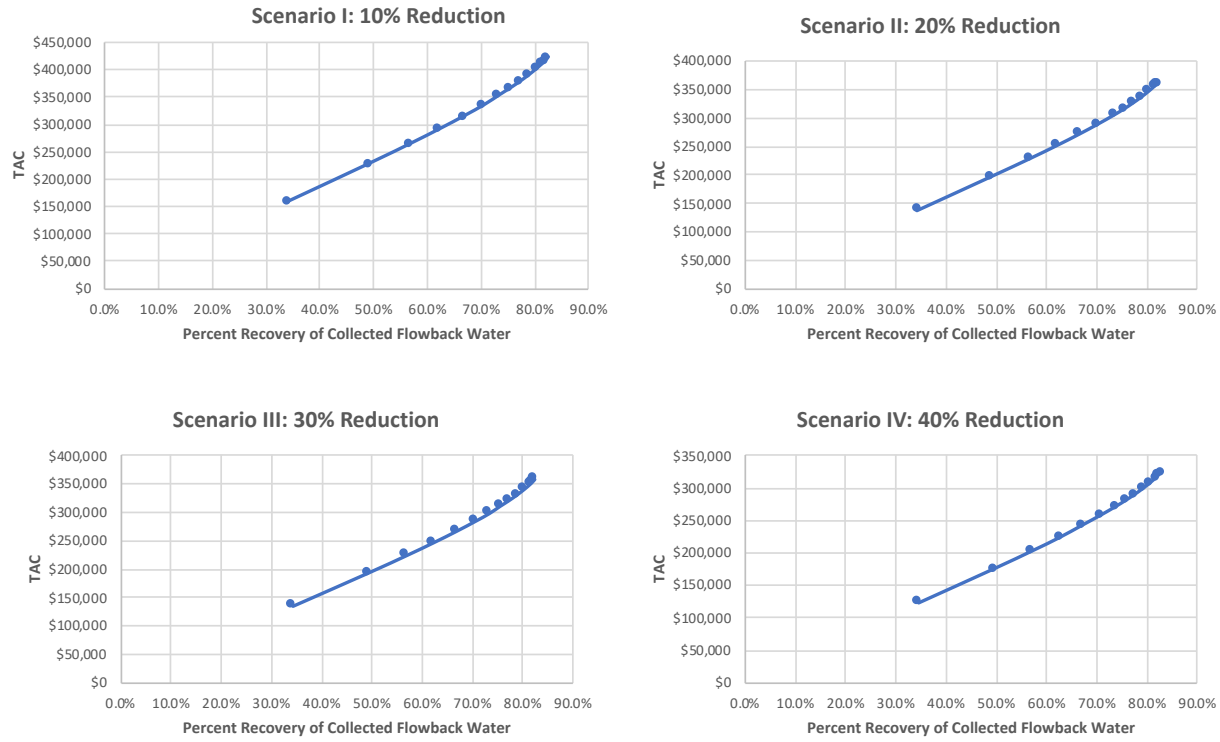

Figure 9. Cumulative TAC and Percent Recovery for Scenarios I-IV

4.3 Scenario Analysis to Assess the Effects of Uncertainty

To determine the economic viability of a project and/or process, it is important to consider the effects of risks and uncertainty. In economic analyses, the use of a sensitivity analysis is advisable as it demonstrates how results can change if one parameter changes. In this analysis, the impact of a reduction in the available amount of fracturing fluid to be injected on the productivity of a stimulated well is investigated.

As discussed in **Section 3.2.1**, the section-based optimization method is an offline optimization-based technique that finds the optimum number of wells n_c, number of fractures per well n_r, and fracture half-length x_f, to maximize the productivity (PI), J_D, of the well [4]. Moreover, for a given amount of proppant, $M_{prop,frac} = 37{,}000\ kg$, if the target average fracture width at the end of pumping is achieved, then the optimal fracture half-length, $x_f = 120\ m$ would also be achieved. As illustrated in **Figure 10,** the desired average fracture width at the end of pumping is attained for each scenario, despite reductions in the total fracturing fluid volume available.

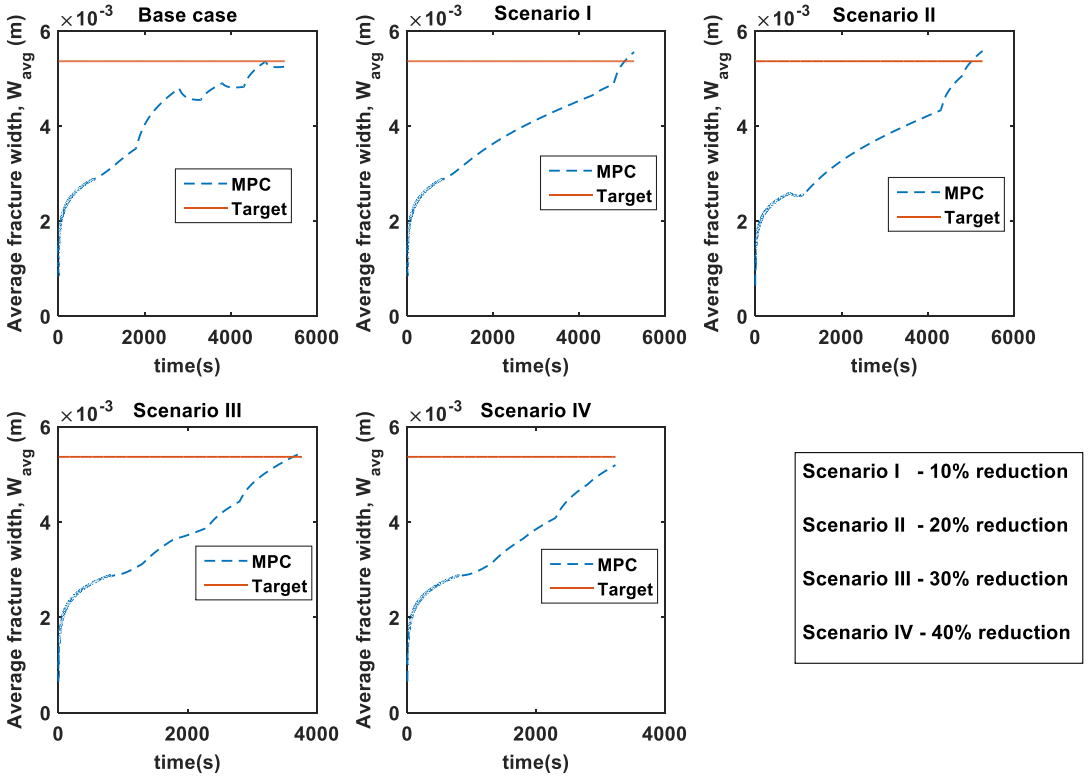

Figure 10. Average Fracture Width During the Hydraulic Fracturing Process Under MPC for Scenarios I-V

Moreover, **Figure 11** illustrates the optimal pumping schedule for each scenario. The reduction in the total volume of water to be injected directly affects the pumping schedule of scenarios III and IV because when there is not sufficient amount of water available, all of the proppant cannot be injected. The only way to inject all of the proppant would be to increase the proppant concentration injected over the time period. However, as described by Eq. (6), there is a limit on the maximum proppant concentration injected. Consequently, the proppant concentration cannot exceed 2 PPGA.

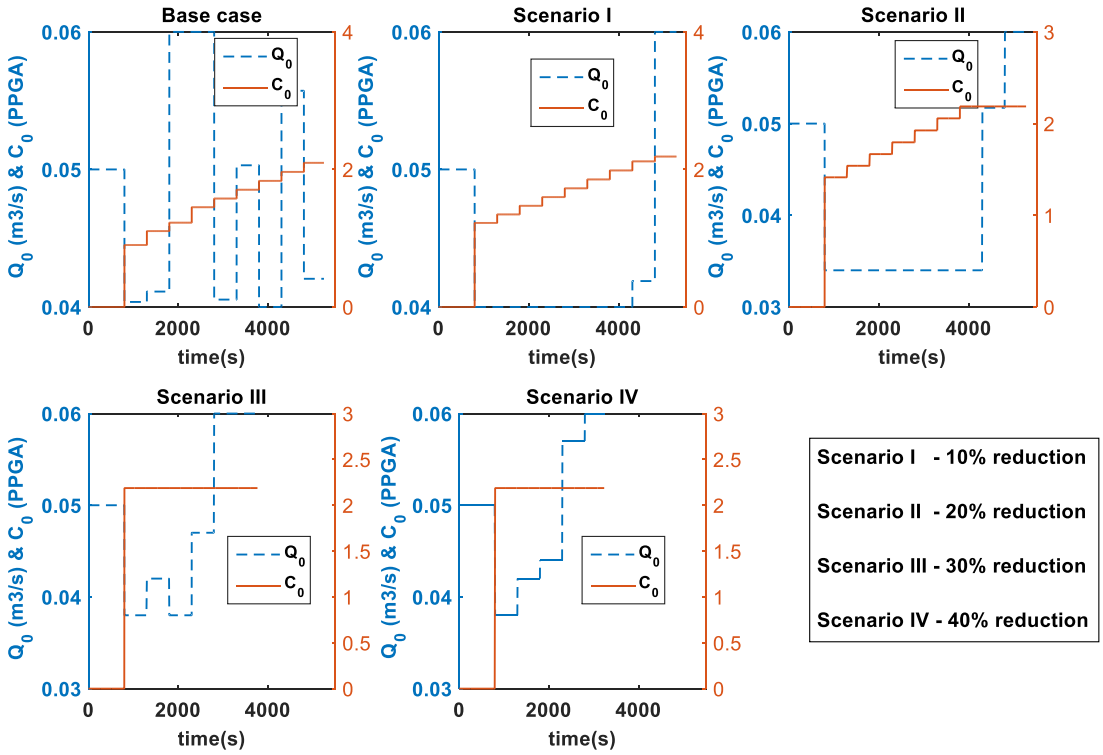

Figure 11. Optimal Pumping Schedule Generated Under MPC for Scenarios I-V

Table 16. Results Obtained for Scenarios I-V

	Total Water Injected, $WR_{prop,frac}$ (m^3)	Total Proppant Injected, $M_{prop,frac}$ (kg)	Fracture Half-Length, x_f (m)	Productivity Index per Well, J_D
Base case	241.09	37,000	120	372.4
10% Reduction	216.98	37,000	120	372.4
20% Reduction	192.90	37,000	120	372.4
30% Reduction	167.86	33,509	105	132.9
40% Reduction	145.11	27,547	87	59.1

As reported in **Table 16,** until 20% reduction in the total fracturing fluid available, the water requirement for well completion can effectively be reduced without any effect on the productivity of the well. For scenarios III and IV, all of the proppant cannot be injected because

of the constraint imposed by Eq. (6). As shown, when the total water available is reduced by 30%, the fracture half-length decreases because there is not enough proppant to cover the remaining part of the fracture. As a result of this, the overall productivity of the stimulated well is reduced by 64%, compared to the base case. A further reduction by 40% leads to a PI of 59.1, or a 84% reduction from the base case.

As discussed in **Sections 4.2 and 4.3,** 82.3% of the collected flowback water is successfully recovered through the TMD system. However, the TAC for the base case is higher than the other scenarios because the actual flowback volume recovered is higher. In other words, more money is spent to recover more flowback water without any benefit to the hydraulic fracturing operation. Although the treated flowback water is sold, profits from recycling are overshadowed by the costs of treatment, transportation etc. In this regard, the main goal should be to maximize profits from the hydraulic fracturing operation instead of maximizing the flowback water recovery. As such, assuming that the amount of water injected is sufficient to create the same stimulated volume of hydrocarbons, the water usage can be reduced by 20%, without affecting the performance of the well. By applying this recommendation, the TAC associated with post-fracturing process becomes $359,228 a 23% reduction from the base case.

4.4 Scenario V: Complete Discharge of the Flowback Water

The treatment and recycle of flowback water are viable solutions to minimize fresh water usage and the negative impacts on the environment. For comparison purposes, complete discharge is considered, meaning the flowback water from the fractured well is directly sent to a disposal unit for deep well injection. **Table 17** shows the cumulative TAC for treatment vs. no treatment for the base case. As shown, an additional $192,917 is spent to directly dispose the flowback water over the course of 14 days. This indicates that the treatment of flowback water is beneficial when we look at the entire framework regarding sustainability. For the present problem, the TAC for complete discharge is high because of the transportation cost to the wastewater disposal site. As mentioned, the data used in this model is taken from flowback water samples associated with shale development in the Marcellus Region. In that region, there are availability and capacity issues related to injection sites. Consequently, the generated flowback water has to be transported over long distances to nearby sites in Ohio or Indiana.

Table 17. Cumulative TAC for Treatment vs. No Treatment

Day*	Cumulative TAC Treatment	Cumulative TAC No Treatment
1	$176,256	$262,938
2	$251,984	$375,903
3	$292,440	$435,201
4	$322,321	$478,101
5	$348,663	$515,038
6	$371,462	$546,178
7	$389,854	$570,527
8	$404,255	$589,244
9	$417,282	$605,311
10	$430,610	$621,212
11	$445,629	$636,782
12	$456,635	$649,039
13	$462,386	$655,167
14	$468,379	$661,296

***Days from the hydraulic fracturing event.

Other than economic and environmental benefits, there are societal benefits as well from the treatment of flowback water. Getting rid of the TMD system indicates that large amounts of untreated flowback water will be disposed via deep well injection. The direct disposal of untreated flowback streams also affects the societal pillar of sustainability. For example, a small leak into the formation could pose risks to animal and human health, as it would result in waste migration and groundwater contamination (Simpson and Lester, 2009). As such, the handling process of flowback water is extremely complex in terms of safety, which is why wastewater treatment is an essential part of the post-fracturing process.

4.5 Environmental Impact Assessment

To analyze and quantify the environmental impact of chemicals in the flowback water collected within the first 14 days, the tool for reduction and assessment of chemical and other environmental impacts (TRACI) is used (Bare, 2011; Bare, 2012; Jiang et al., 2014). The TRACI framework, developed by the Environmental Protection Agency (EPA) characterizes factors for sustainability metrics to quantify the potential effects of ozone depletion, climate change,

acidification, eutrophication, smog formation, human health impact, and ecotoxicity. It is an Excel® based tool where each compound can be identified by substance names and/or their chemical abstract service numbers (CAS). The corresponding characterization factors of each chemical is given based on their respective impacts (Bare, 2012). In this research, the focus is on impact categories related to fresh water pollution such as: eutrophication potential (in kg of N equivalent), freshwater ecotoxicity potential (in CTUeco per kg), carcinogenic potential (in CTUcancer per kg) and noncarcinogenic potential (in CTUnoncancer per kg) (Bare, 2012; Jiang et al., 2014). The following equation is used to calculate the environmental impact of each of the above-mentioned categories.

$$Potential\ Environmental\ Impact = \sum Mass\ of\ Chemical * TRACI\ Characterization\ Factor \quad (63)$$

The average and median concentrations of chemicals present in flowback water for the base case are reported in **Table 18.** It is important to note that some major contributing chemicals present in flowback water are not listed in **Table 18 and 19** because they do not have an assigned characterization factor in TRACI. These include but are not limited to: bromide, calcium, chloride, magnesium, and strontium.

Table 18. The Average and Median Values of Chemical Concentrations in the Collected Flowback Water (Revised from Jiang et al., 2014)

CAS #	Parameter	Unit	Average	Median
95636	1,2,4-Trimethylbenzene	ug/L	90	1
108678	1,3,5-Trimethylbenzene	ug/L	74	0
78933	2-Butanone	ug/L	0	0
91576	2-Methylnaphthalene	ug/L	0	0
95487	2-Methylphenol	ug/L	1	0
88744	2-Nitroaniline	ug/L	0	0
67630	2-Propanol	mg/L	68	0
7005723	4-Chlorophenyl Phenyl Ether	ug/L	0	0
108101	4-Methyl-2-pentanone (MIBK)	ug/L	0	0
83329	Acenaphthene	ug/L	0	0
64197	Acetic Acid	mg/L	17	0
67641	Acetone	ug/L	489	18

Table 18. (Continued)

CAS #	Parameter	Unit	Average	Median
98862	Acetophenone	ug/L	2	0
NH4-N	Ammonia Nitrogen	mg/L	92	0
62533	Aniline	ug/L	0	0
7440382	Arsenic	ug/L	24	0
7440393	Barium	ug/L	1,625,847	686,000
71432	Benzene	ug/L	221	0
56553	Benzo(a)anthracene	ug/L	0	0
50328	Benzo(a)pyrene	ug/L	0	0
100516	Benzyl Alcohol	ug/L	1	0
BOD	Biological Oxygen Demand (BOD)	mg/L	449	144
111444	bis(2-Chloroethyl) Ether	ug/L	1	0
117817	bis(2-Ethylhexyl) Phthalate	ug/L	6	2
74839	Bromomethane	ug/L	8	0
71363	Butyl Alcohol	mg/L	3	0
85687	Butyl Benzyl Phthalate	ug/L	0	0
75150	Carbon Disulfide	ug/L	35	0
COD	Chemical Oxygen Demand (COD)	mg/L	5,402	4,870
67663	Chloroform	ug/L	0	0
7440508	Copper	ug/L	536	0
84742	Di-n-butyl Phthalate	ug/L	2	0
117840	Di-n-octyl Phthalate	ug/L	1	0
53703	Dibenz(a,h)anthracene	ug/L	1	0
132649	Dibenzofuran	ug/L	0	0
84662	Diethyl Phthalate	ug/L	2	0
122394	Diphenylamine	ug/L	0	0
64175	Ethanol	mg/L	37	0
100414	Ethylbenzene	ug/L	41	0
107211	Ethylene Glycol	mg/L	52	0
206440	Fluoranthene	ug/L	0	0
86737	Fluorene	ug/L	0	0
118741	Hexachlorobenzene	ug/L	0	0
98828	Isopropyl Benzene	ug/L	8	0
7439921	Lead	ug/L	71	0
67561	Methanol	mg/L	113	0
75092	Methylene Chloride	ug/L	0	0

Table 18. (Continued)

CAS #	Parameter	Unit	Average	Median
86306	N-Nitroso Diphenylamine	ug/L	0	0
91203	Naphthalene	ug/L	14	0
Nitrate-N	Nitrate as N	mg/L	0	0
Nitrate-Nitrite N	Nitrate-Nitrite	mg/L	0	0
Nitrite-N	Nitrite as N	mg/L	8	6
85018	Phenanthrene	ug/L	0	0
108952	Phenol	ug/L	2	0
99876	p-Isopropyl Toluene	ug/L	4	0
57556	Propylene Glycol	mg/L	103	0
129000	Pyrene	ug/L	0	0
110861	Pyridine	ug/L	214	10
135988	sec-Butylbenzene	ug/L	4	0
108883	Toluene	ug/L	511	1
7723140	Total Phosphorous	mg/L	1	0
16065831	Trivalent Chrom	ug/L	6	0
1330207	Xylenes (total)	ug/L	438	4
7440666	Zinc	ug/L	705	0

Table 19. Potential Environmental Toxicity of the Average Mass of Chemicals Present in the Collected Flowback Water

Parameter	Average Mass of Chemical (kg)	Eutrophication (kg N eq)	Ecotoxicity (CTUeco)	Carcinogenic (CTUcancer)	Non-Carcinogenic (CTUnoncancer)
1,2,4-Trimethylbenzene	0.23047	0	165.1	1.263E-09	0
1,3,5-Trimethylbenzene	0.18949	0	56.6	0	0
2-Butanone	0	0	0	0	0
2-Methylnaphthalene	0	0	0	0	0
2-Methylphenol	2.56E-03	0	1.5097	0	5.122E-10
2-Nitroaniline	0	0	0	0	0
2-Propanol	174.1	0	428.9	0	0
4-Chlorophenyl Phenyl Ether	0	0	0	0	0
4-Methyl-2-pentanone (MIBK)	0	0	0	0	0
Acenaphthene	0	0	0	0	0

Table 19. (Continued)

Parameter	Average Mass of Chemical (kg)	Eutrophication (kg N eq)	Ecotoxicity (CTUeco)	Carcinogenic (CTUcancer)	Non-Carcinogenic (CTUnoncancer)
Acetic Acid	43.5	0	2169.7	0	0
Acetone	1.2522	0	1.5193	0	7.338E-09
Acetophenone	0.005122	0	0.37029	0	8.553E-11
Ammonia Nitrogen	235.6	235.6	0	0	0
Aniline	0	0	0	0	0
Arsenic	0.06146	0	2482.3	2.268E-05	0.001679
Barium	4163.4	0	6,353,834.7	0	0.40885
Benzene	0.56593	0	37.3	1.369E-07	3.475E-08
Benzo(a)anthracene	0	0	0	0	0
Benzo(a)pyrene	0	0	0	0	0
Benzyl Alcohol	0.002561	0	0.51328	0	0
Biological Oxygen Demand (BOD)	1149.8	57.5	0	0	0
bis(2-Chloroethyl) Ether	0.002561	0	0.15396	1.631E-08	0
bis(2-Ethylhexyl) Phthalate	0.01536	0	4.95	1.346E-09	1.875E-08
Bromomethane	0.02049	0	32.51	0	1.251E-06
Butyl Alcohol	7.682	0	42.37	0	2.881E-07
Butyl Benzyl Phthalate	0	0	0	0	0
Carbon Disulfide	0.08962709	0	13.8	0	3.361E-06
Chemical Oxygen Demand (COD)	13,833.3	691.7	0	0	0
Chloroform	0	0	0	0	0
Copper	1.3726	0	75,831.4	0	1.185E-06
Di-n-butyl Phthalate	0.005122	0	32.36	0	5.839E-10
Di-n-octyl Phthalate	0.002561	0	0.07721	0	0
Dibenz(a,h)anthracene	0.002561	0	7.4848	7.836E-08	0
Dibenzofuran	0	0	0	0	0
Diethyl Phthalate	0.005122	0	2.1664	0	6.965E-11
Diphenylamine	0	0	0	0	0
Ethanol	94.7	0	295.01	2.407E-07	0
Ethylbenzene	0.10499	0	18.362	4.966E-09	3.916E-09
Ethylene Glycol	133.2	0	184.3	0	2.024E-06
Fluoranthene	0	0	0	0	0
Fluorene	0	0	0	0	0
Hexachlorobenzene	0	0	0	0	0
Isopropyl Benzene	0.020486	0	13.625	0	5.675E-10
Lead	0.18182	0	68.128	6.218E-08	2.183E-05
Methanol	289.4	0	765.9	0	3.039E-06
Methylene Chloride	0	0	0	0	0
N-Nitroso Diphenylamine	0	0	0	0	0

Table 19. (Continued)

Parameter	Average Mass of Chemical (kg)	Eutrophication (kg N eq)	Ecotoxicity (CTUeco)	Carcinogenic (CTUcancer)	Non-Carcinogenic (CTUnoncancer)
Naphthalene	0.035851	0	66.958	3.729E-08	1.083E-08
Nitrate as N	0	0	0	0	0
Nitrate-Nitrite	0	0	0	0	0
Nitrite as N	20.486	20.486	0	0	0
Phenanthrene	0	0	0	0	0
Phenol	0.005122	0	4.779	0	7.426E-10
p-Isopropyl Toluene	0.010243	0	3.238	0	0
Propylene Glycol	263.8	0	243.4	0	3.825E-05
Pyrene	0	0	0	0	0
Pyridine	0.548005	0	30.902	1.255E-06	3.809E-06
sec-Butylbenzene	0.010243	0	0	0	0
Toluene	1.30856	0	73.18	4.305E-09	2.329E-08
Total Phosphorous	2.56077	18.668	0	0	0
Trivalent Chromium	0.01537	0	19.891	0	4.656E-11
Xylenes (total)	1.12162	0	86.851	4.352E-09	1.761E-08
Zinc	1.8053	0	69,658.5	0	0.002313

The TRACI tool is used to quantify the environmental toxicity mitigated when the flowback water is treated via a thermal membrane distillation system. Impacts from the average and median concentration of the compounds are shown in **Table 20.** Eutrophication is characterized as the enrichment of nutrients (nitrates, phosphates) in an aquatic ecosystem that contributes to the excessive growth of plants and algae and the death of animal life due to the lack of oxygen (Bare, 2012; Chislock et al., 2013). The eutrophication potential mostly results from chemical oxygen demand (COD), ammonia nitrogen, and biological oxygen demand (BOD) impacts, in descending order. Although substances such as copper, zinc, and arsenic impact fresh water ecotoxicity, barium with 6,353,834.7 CTUeco accounts for roughly 97% of the total potential.

Barium, which is characterized as a signature chemical for tracing flowback water and its impact on the environment, has an average and median concentration of 1,626 mg/L and 686 mg/L respectively. These values are comparable to the literature in which barium concentration ranges from 0.24 mg/L and 2,580 mg/L (Vidic, 2015; Ziemkiewicz and He, 2015). Moreover, the carcinogenic and non-carcinogenic environmental potentials are also included in **Table 20**. Although arsenic, pyridine, benzene, and ethanol impact the carcinogenic potential, the score for

this impact category is low because naturally occurring radioactive material (NORM), chloride, and bromide which may have potential human health cancer toxicity do not have a characterization factor in TRACI (Jiang et al., 2014). In terms of non-carcinogenic potential, barium accounts for 99% of the total environmental impact. Other contributing chemicals include but are not limited to: arsenic, propylene glycol, and zinc.

Table 20. Potential Environmental Toxicity of the Average and Median Mass of the Chemicals Present in the Collected Flowback Water

	Eutrophication (kg N eq)	Ecotoxicity (CTUeco)	Carcinogenic (CTUcancer)	Non-carcinogenic (CTUnoncancer)
Average Chemical Impact	1,024	6,506,679	2.452E-05	0.41292
Median Chemical Impact	657	2,680,904	5.915E-08	0.17251

5. CONCLUSION

The exploration and production of shale oil and gas through hydraulic fracturing has allowed the United States to gradually become energy independent. However, this newfound independence has come with a cost to water resources and the environment. Over the past few years, several studies have focused on water management and treatment strategies to overcome these consequences. As such, this work proposed a new control framework that integrates sustainability considerations of the post-fracturing process into the hydraulic fracturing process. Through the methodology and model proposed, the economy of the wastewater management process that consists of hydraulic fracturing, storage, transportation, and water treatment, is successfully estimated and some valuable insights could be obtained.

First, the dynamic input-output model guaranteed a 32% flowback water collection from the total fracturing volume injected. Of the 32% water stream that emerged to the surface shortly after well completion, 82.3% was successfully recovered through treatment via a thermal membrane distillation system. Second, the productivity index of stimulated wells showed significant sensitivity to water reductions of 30% and above. This indicates an opportunity to reduce the water footprint of the hydraulic fracturing process by 20%, which will decrease the annualized costs of the post-fracturing process, with no impact on the productivity of the stimulated well. Note that any reduction in the total fracturing fluid available assumes that the amount of water injected is sufficient to create the same stimulated volume. Third, complete discharge of the flowback water demonstrated that the benefits of wastewater treatment were not only from an environmental and societal point of view, but also economic point of view, as treatment reduces TAC by 30%. Finally, when the flowback water was treated via a thermal membrane distillation system, environmental toxicity was mitigated which showed another importance of optimal wastewater management.

REFERENCES

Bai, B., Goodwin, S., Carlson, K., 2013. Modeling of Frac Flowback and Produced Water Volume from Wattenberg Oil and Gas Field. Journal of Petroleum Science and Engineering 108, 383-392.

Bare, J., 2011. TRACI 2.0: The Tool for the Reduction and Assessment of Chemical and Other Environmental Impacts 2.0. Clean Technologies and Environmental Policy 13(5).

Bare, J., 2012.User's Manual: Tool for the Reduction and Assessment of Chemical and Other Environmental Impacts (TRACI) 2.1. United States Environmental Protection Agency: Sustainable Technology Division, Systems Analysis Branch.

Boschee, P., 2014. Produced and Flowback Water Recycling and Reuse: Economics, Limitations, and Technology. Oil and Gas Facilities 3 (01), 16-21.

Chislock, M. F., Doster, E., Zitomer, R. A., Wilson, A. E., 2013. Eutrophication: Causes, Consequences, and Controls in Aquatic Ecosystems. Nature Education Knowledge 4(4), 10.

Clark, C. E., Horner, R. M., Harto, C. B., 2013. Life Cycle Water Consumption for Shale Gas and Conventional Natural Gas. Environ. Sci. Technol 47 (20), 11829−11836.

Collins, G., 2016. A Simple Model for Pricing and Trading Produced Water in the Permian Basin. Rice University's Baker Institute for Public Policy.

Economides, M. J., Obligney, R. E., Valko, P. P, 2002. Unified Fracture Design. CA: Orsa Press.

Elsayed, N. A., Barrufet, M. A., El-Halwagi, M. M., 2013. Integration of Thermal Membrane Distillation Networks with Processing Facilities. Industrial & Engineering Chemistry Research 53(13), 5284-5298.

Elsayed, N. A., Barrufet, M. A., Eljack, F. T., El-Halwagi, M. M., 2015. Optimal Design of Thermal Membrane Distillation System for the Treatment of Shale Gas Flowback Water. Int J Membr Sci Technol 2, 1-9.

FracFocus: Chemical Disclosure Registry, 2012. Chemical Use in Hydraulic Fracturing. Retrieved from: https://fracfocus.org/water-protection/drilling-usage.

Gao, J., You, F., 2015a. Optimal Design and Operations of Supply Chain Networks for Water Management in Shale Gas Production: MILFP Model and Algorithms for the Water Energy Nexus. AIChE Journal 61 (4), 1184−1208.

Gao, J., You, F., 2015b. Deciphering and Handling Uncertainty in Shale Gas Supply Chain Design and Optimization: Novel Modeling Framework and Computationally Efficient Solution Algorithm. AIChE Journal 61 (11), 3739−3755.

Gu, Q., Hoo, K. A., 2014. Evaluating the Performance of a Fracturing Treatment Design. Industrial & Engineering Chemistry Research 53 (25), 10491-10503.

Hayes, T., 2009. Sampling and Analysis of Water Streams Associated with the Development of Marcellus Shale Gas. Marcellus Shale Initiative Publications Database, 10.

Health Canada, 1991. Total Dissolved Solids (TDS). Health Canada. Retrieved from: http://health.canada.ca/publications/healthy-living-vie-saine/water-dissolved-solids-matieres-dissoutes-eau/alt/water-dissolved-solids-matieres-dissoutes-eau-eng.pdf.

Henderson, C., Acharya, H., Matis, H., Kommepalli, H., Moore, B., Wang, H., 2011. Cost Effective Recovery of Low-TDS Frac Flowback Water for Re-use. General Electric Company.

Islam, S. M., Sadiq, R., Rodriguez, M. J., Najjaran, H., Hoorfar, M., 2014. Reliability Assessment for Water Supply Systems Under Uncertainties. Journal of Water Resources Planning and Management 140 (4), 468−479.

Jiang, M., Hendrickson, C. T., VanBriesen, J. M., 2014. Life Cycle Water Consumption and Wastewater Generation Impacts of a Marcellus Shale Gas Well. Environ. Sci. Technol 48 (3), 1911−1920.

Khor, C. S., Chachuat, B., & Shah, N. 2014. Fixed-flowrate Total Water Network Synthesis Under Uncertainty with Risk Management. Journal of Cleaner Production 77, 79-93.

Lira-Barragan, L.F., Ponce-Ortega, J.M., Guillen-Gosalbez, G., El-Halwagi, M.M., 2015. Optimal Water Management Under Uncertainty for Shale Gas Production. Industrial & Engineering Chemistry Research 55 (5), 1322-1335.

Liu, S., Valkó, P. P., 2017. Optimization of Spacing and Penetration Ratio for Infinite-Conductivity Fractures in Unconventional Reservoirs: A Section-Based Approach. SPE Journal.

Nápoles-Rivera, F., Rojas-Torres, M., H. R., Ponce-Ortega, J. M., Serna-Gonzales, M., El-Halwagi, M.M., 2015. Optimal Design of Macroscopic Water Networks Under Parametric Uncertainty. Journal of Cleaner Production 88, 172-184.

Narasingam, A., Kwon, J. S. I., 2017. Development of Local Dynamic Mode Decomposition with Control: Application to Model Predictive Control of Hydraulic Fracturing. Computers & Chemical Engineering 106, 501-511.

Narasingam, A., Siddhamshetty, P., Kwon, J. S. I., 2017. Temporal Clustering for Order Reduction of Nonlinear Parabolic PDE Systems with Time-dependent spatial Domains: Application to a Hydraulic Fracturing Process. AIChE Journal 63(9), 3818-3831.

Narasingam, A., Siddhamshetty, P., Kwon, J. S. I., 2018. Handling Spatial Heterogeneity in Reservoir Parameters Using Proper Orthogonal Decomposition Based Ensemble Kalman Filter for Model-Based Feedback Control of Hydraulic Fracturing. Industrial & Engineering Chemistry Research 57(11), 3977-3989.

NSF: Live Safer. About Total Dissolved Solids in Drinking Water. Retrieved from: https://www.nsf.org/newsroom_pdf/cons_sodium_tds.pdf.

Pangarkar, B. L., Sane, M. G., Guddad, M., 2011. Reverse Osmosis and Membrane Distillation for Desalination of Groundwater: A Review. ISRN Material Science.

Rosemblum, J., Nelson, A. W., Ruyle, B., Schultz, M. K., Ryan, J. N., Linden, K. G., 2017. Temporal Characterization of Flowback and Produced Water Quality from a Hydraulically Fractured Oil and Gas Well. Science of the Total Environment 596, 369-377.

Siddhamshetty, P., Yang, S., Kwon, J. S. I., 2017. Modeling of Hydraulic Fracturing and Designing of Online Pumping Schedules to Achieve Uniform Proppant Concentration in Conventional Oil Reservoirs. Computers & Chemical Engineering.

Siddhamshetty, P., Kwon, J. S. I., Liu, S., Valkó, P. P., 2018. Feedback Control of Proppant Bank Height During Hydraulic Fracturing for Enhanced Productivity in Shale Formations. AIChE Journal 64 (5), 1638-1650.

Siddhamshetty, P., Wu, K., Kwon, J. S. I., 2018. Optimization of Simultaneously Propagating Multiple Fractures in Hydraulic Fracturing to Achieve Uniform Growth Using Data-Based Model Reduction. Chemical Engineering Research and Design 136, 675-686.

Sidhu, H. S., Siddhamshetty, P., Kwon, J. S. I., 2018. Approximate Dynamic Programming Based Control of Proppant Concentration in Hydraulic Fracturing. Mathematics 6, 132.

Simpson, H., Lester, S., 2009. Deep Well Injection: an Explosive Issue. Center for Health, Environment, and Justice.

US Environmental Protection Agency. (2016). Hydraulic Fracturing for Oil and Gas: Impacts from the Hydraulic Fracturing Water Cycle on Drinking Water Resources in the United States.

Vidic, R., 2015. Sustainable Management of Flowback Water during Hydraulic Fracturing of Marcellus Shale for Natural Gas Production. University of Pittsburgh, PA (United States).

Wang, Z., Krupnick, A., 2013. A Retrospective Review of Shale Gas Development in the United States: What Led to the Boom?.

Water Research Center, 2014. Total Dissolved Solids and Water Quality. Retrieved from: https://www.water-research.net/index.php/water-treatment/tools/total-dissolved-solids.

Water Technology: Solutions for Industrial Water Management, 2016. Fracking Water Treatment Technologies. Retrieved from: https://www.watertechonline.com/hydraulic-fracturing- water-technologies/.

Yang, L., Grossmann, I. E., Manno, J., 2014. Optimization Models for Shale Gas Water Management. AIChE Journal 60 (10), 3490-3501.

Yang, S., Siddhamshetty, P., Kwon, J. S. I., 2017. Optimal Pumping Schedule Design to Achieve a Uniform Proppant Concentration Level in Hydraulic Fracturing. Computers & Chemical Engineering 101, 138-147.

Zhiltsov, S. S., Shemenov, A.V., 2016. Shale Gas: History of Development. In Shale Gas: Ecology, Politics, Economy. Springer, Cham. 9-16.

Ziemkiewicz, P. F., He, Y. T., 2015. Evolution of Water Chemistry During Marcellus Shale Gas Development: A Case Study in West Virginia. Chemosphere 134, 224-231.

Zuppann, C.W., Steinmetz, J. C., 2014. Hydraulic Fracturing: An Indiana Assessment.